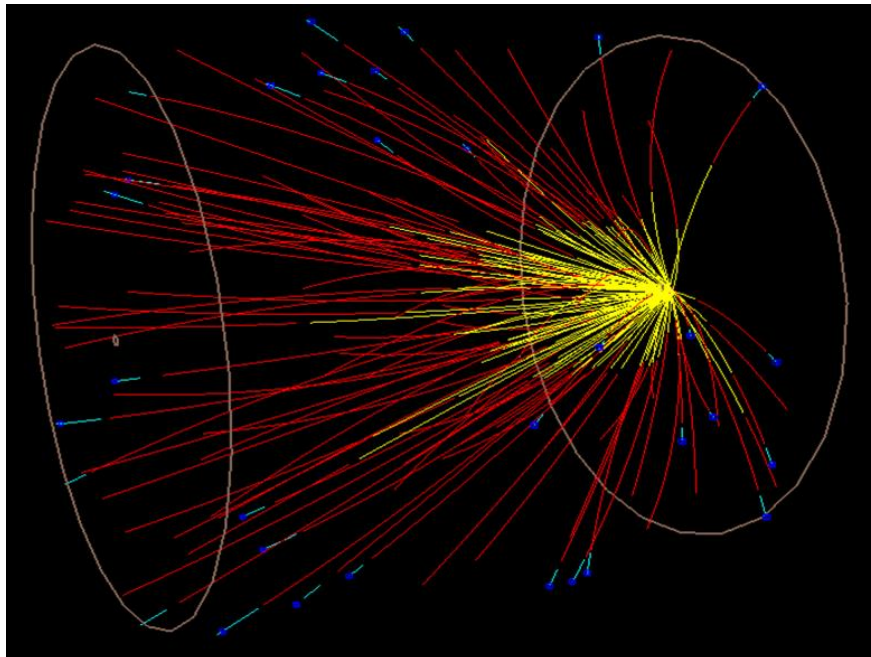
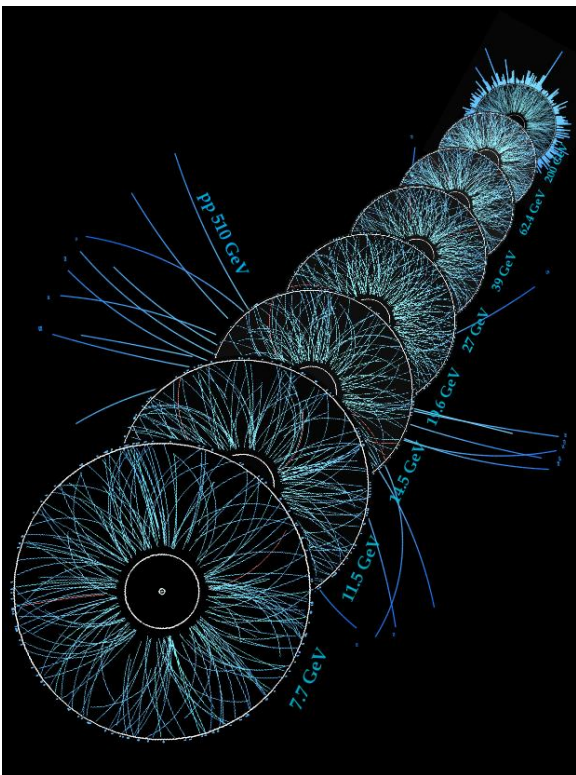
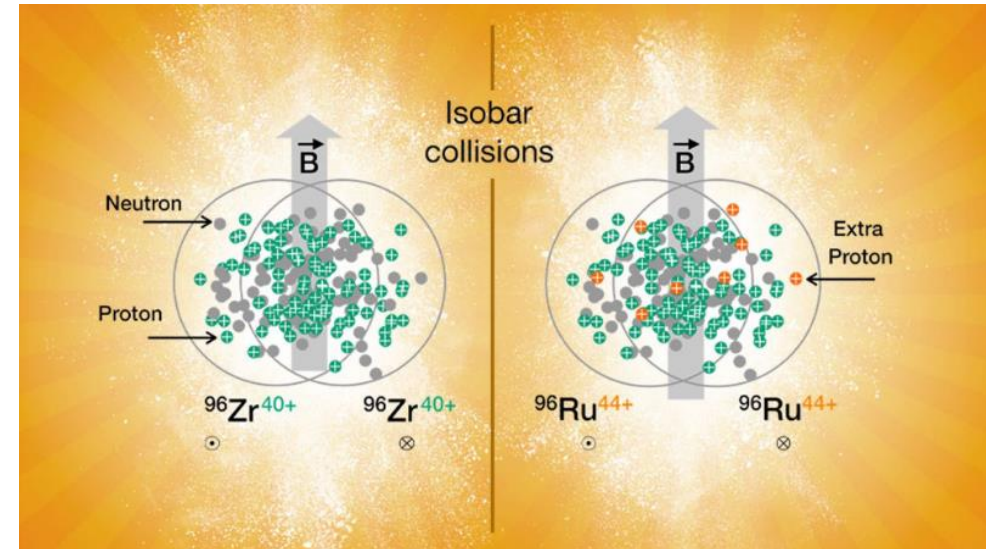


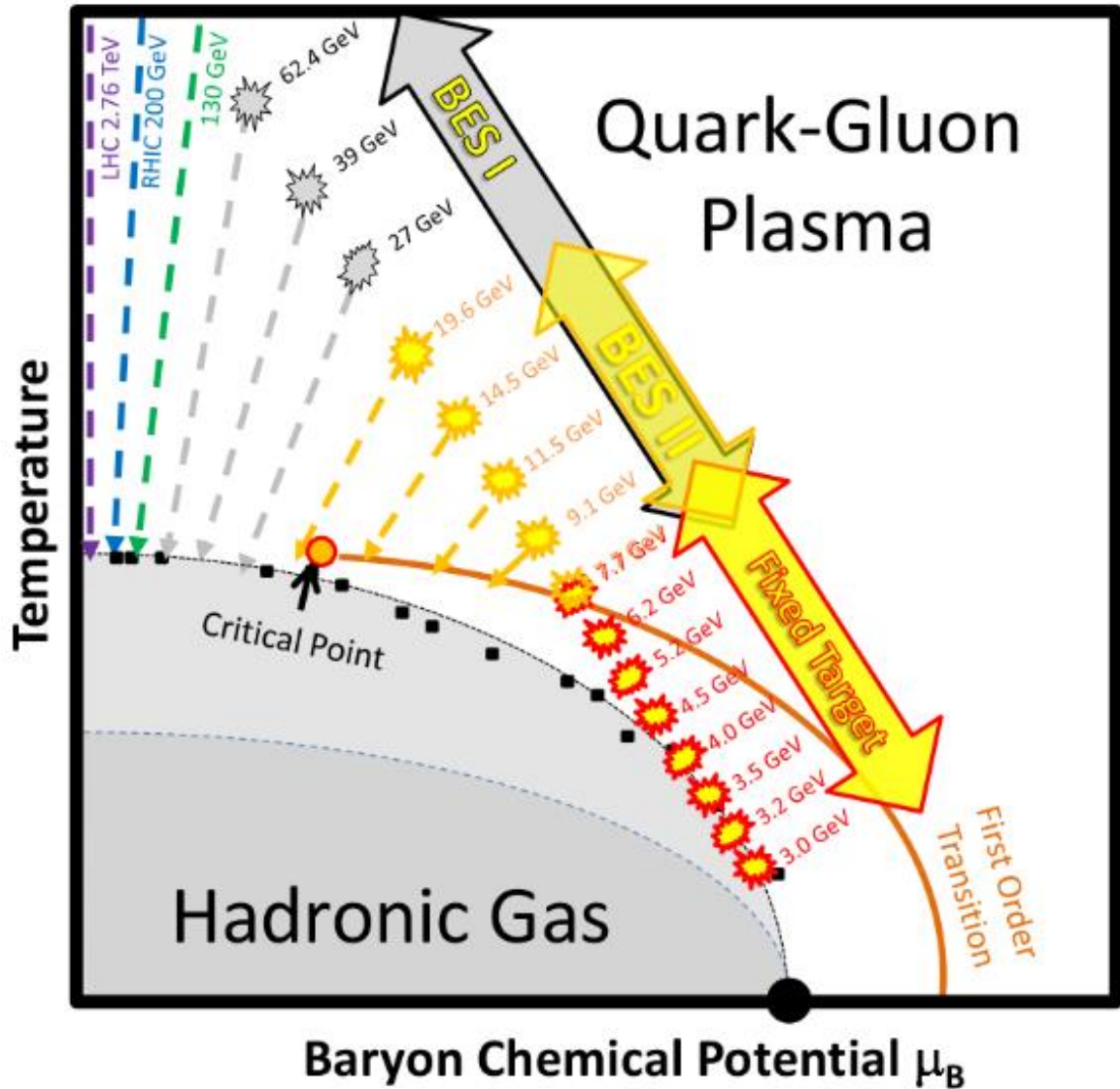
Results from the Beam Energy Scan Program at STAR



Grigory Nigmatkulov



STAR ☆ BES-I → BES-II and FXT

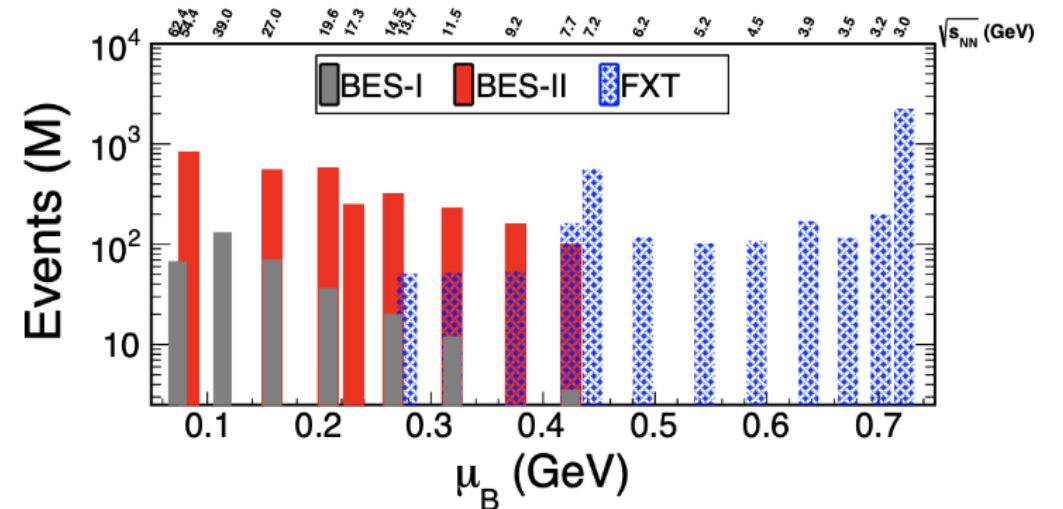


BES-I:

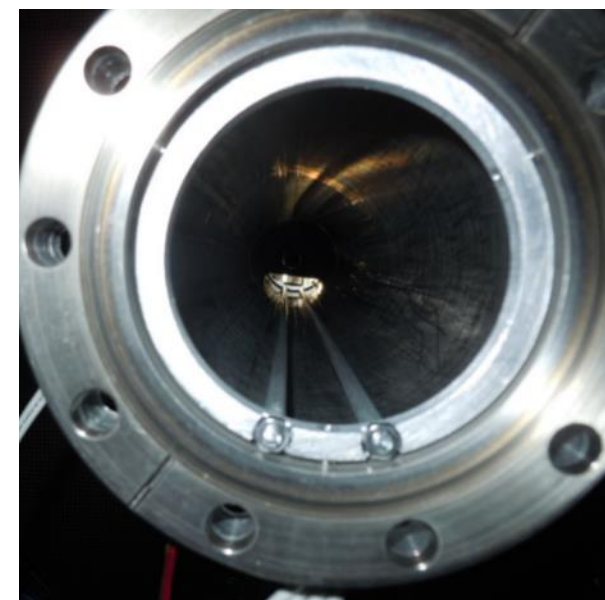
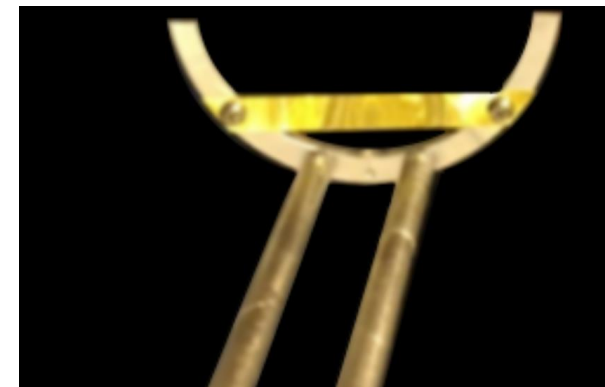
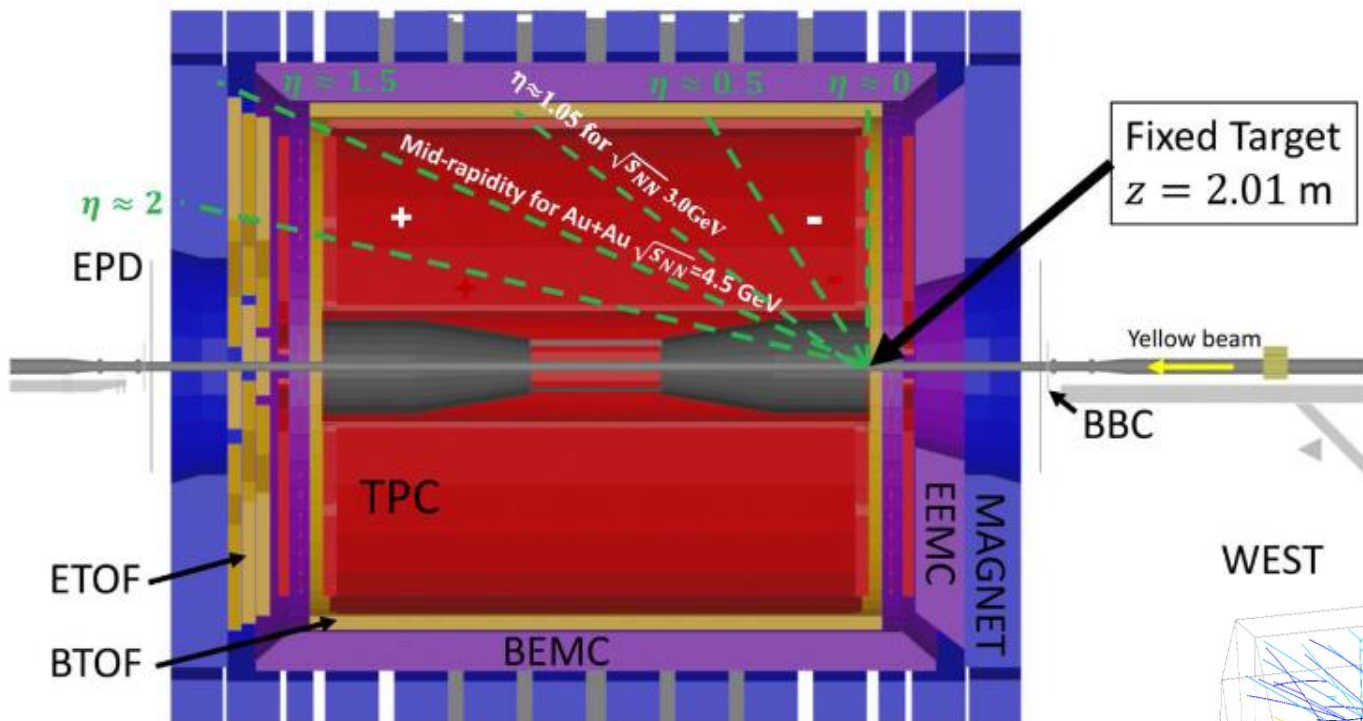
- Search for the QGP turn-off signatures
- Search for the first-order phase transition
- Search for the critical point

BES-II and fixed-target (FXT) program:

- Need higher statistics (≥ 10 times than in BES-I) for precise measurements
- Detector upgrades (increased acceptance and PID capabilities)
- Access to energies $\sqrt{s_{NN}} < 7.7$ GeV via FXT

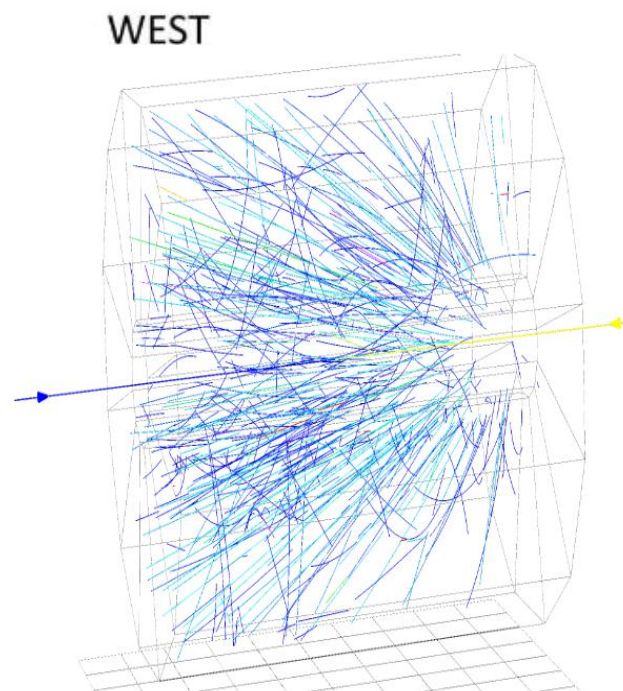


STAR ☆ The Fixed-target (FXT) Setup



Gold target:

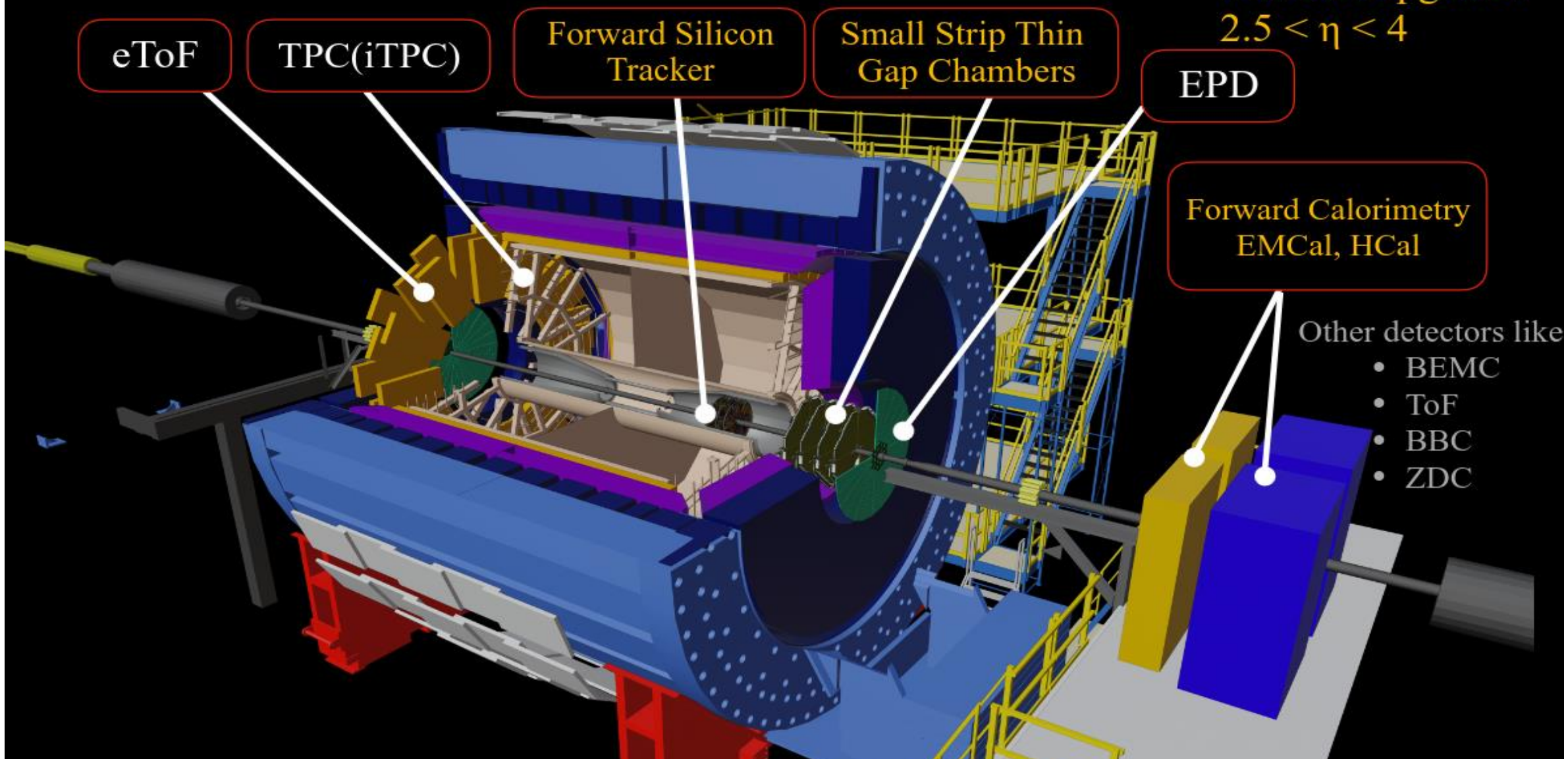
- 2 cm below nominal beam axis
- 2 m from center of STAR
- 250 μm foil





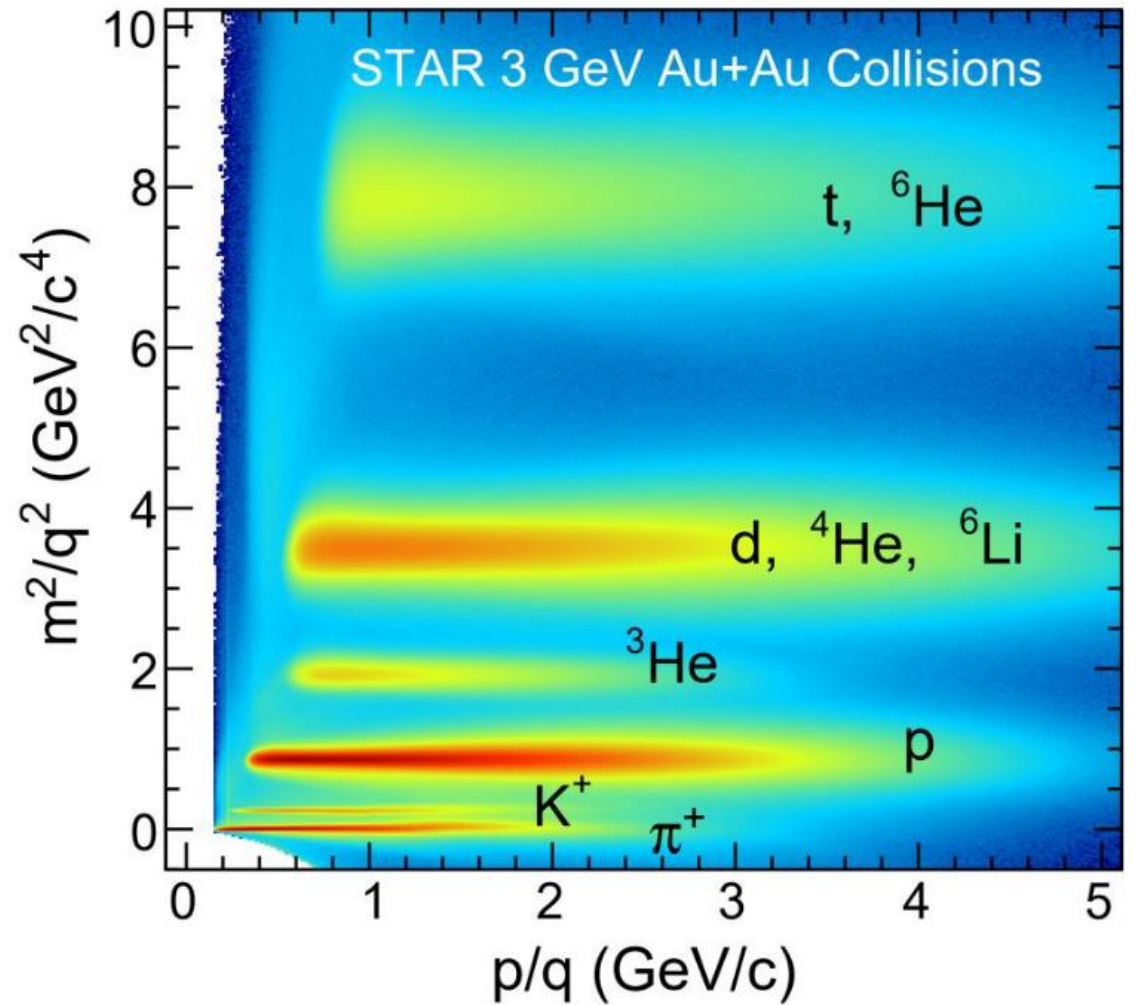
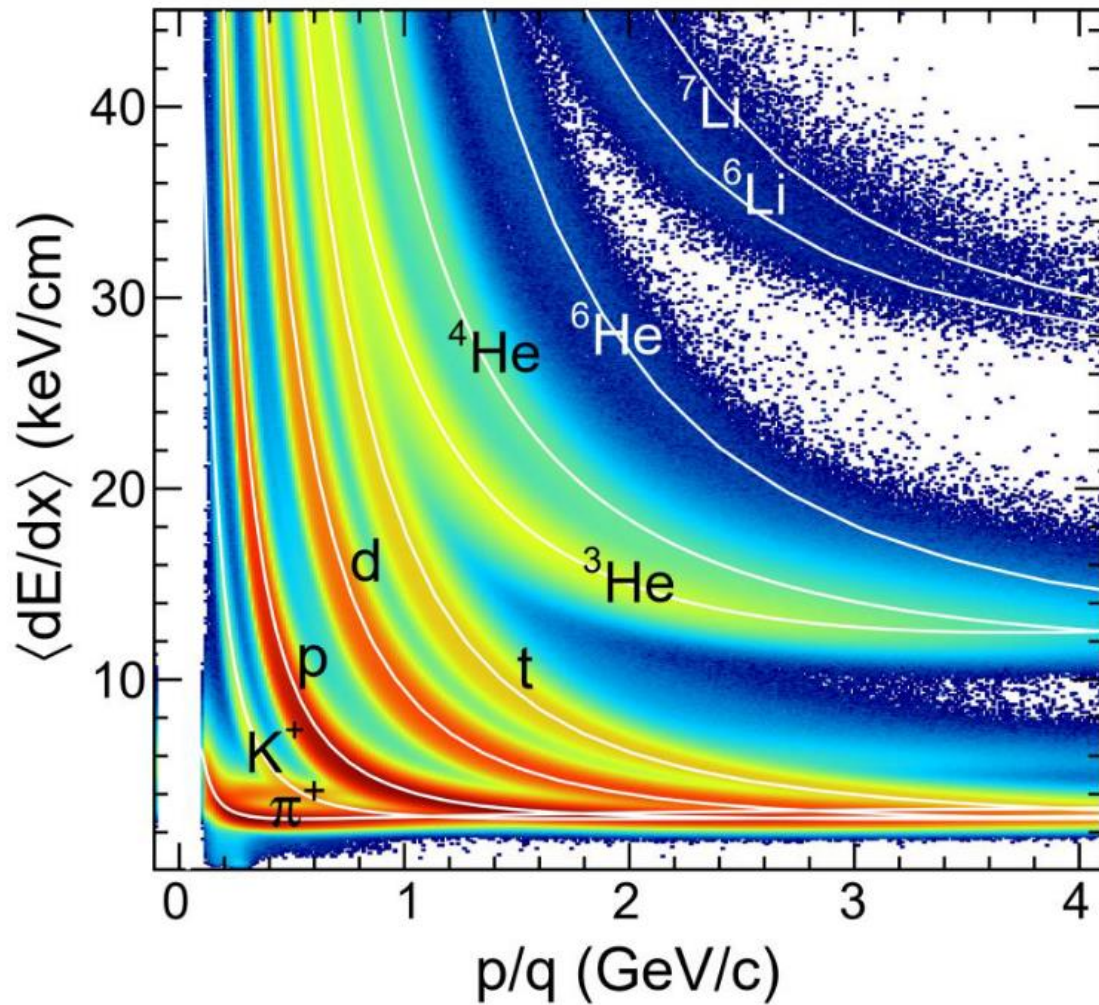
STAR detector

BES-II upgrade
Forward upgrade:
 $2.5 < \eta < 4$





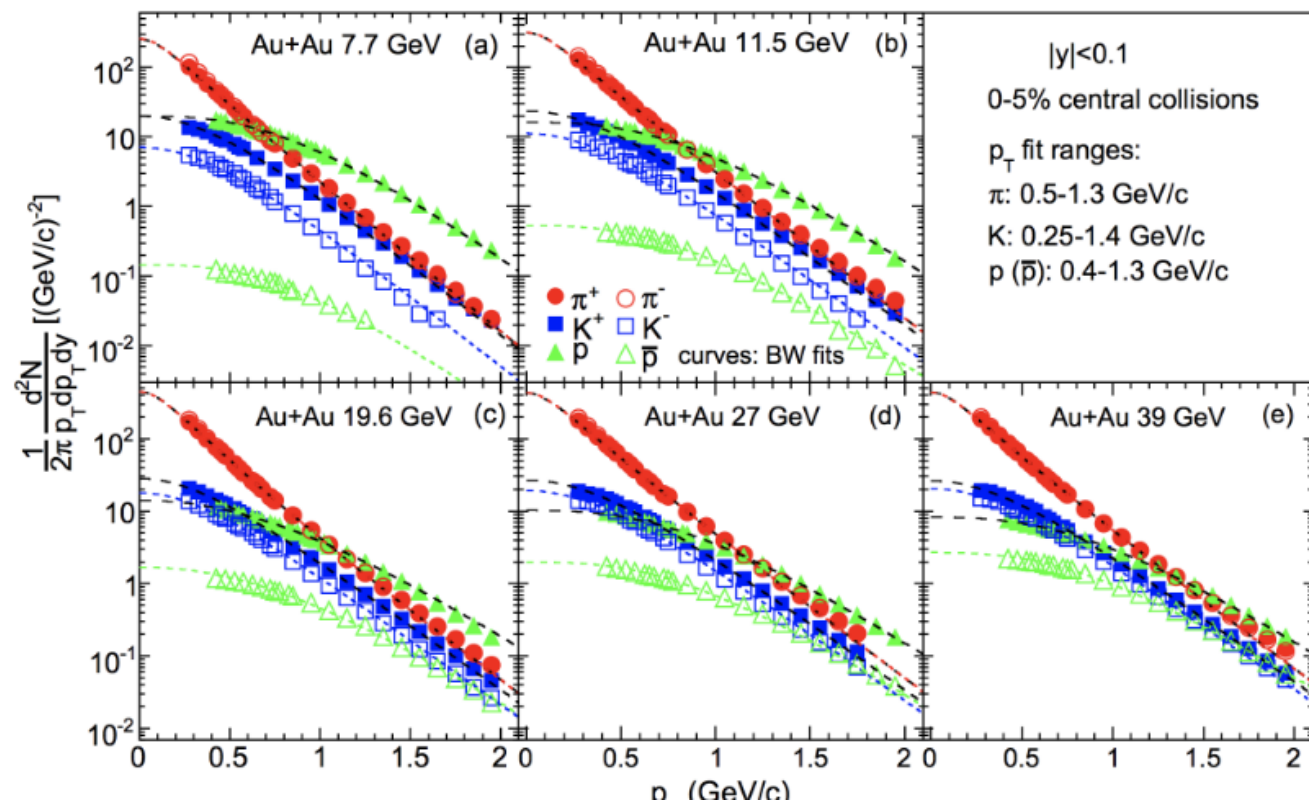
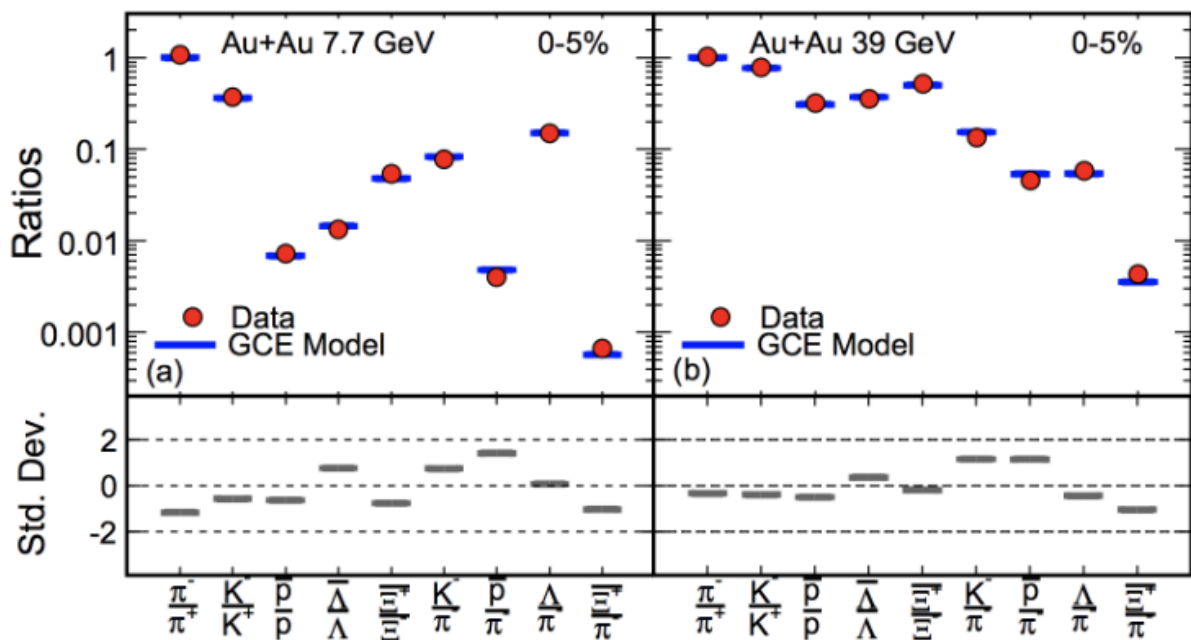
$\sqrt{s_{NN}}$ (GeV)	Beam Energy (GeV/nucleon)	Collider or Fixed Target	$y_{center\ of\ mass}$	μ^B (MeV)	Run Time (days)	No. Events Collected (Request)	Date Collected
200	100	C	0	25	2.0	138 M (140 M)	Run-19
27	13.5	C	0	156	24	555 M (700 M)	Run-18
19.6	9.8	C	0	206	36	582 M (400 M)	Run-19
17.3	8.65	C	0	230	14	256 M (250 M)	Run-21
14.6	7.3	C	0	262	60	324 M (310 M)	Run-19
13.7	100	FXT	2.69	276	0.5	52 M (50 M)	Run-21
11.5	5.75	C	0	316	54	235 M (230 M)	Run-20
11.5	70	FXT	2.51	316	0.5	50 M (50 M)	Run-21
9.2	4.59	C	0	372	102	162 M (160 M)	Run-20+20b
9.2	44.5	FXT	2.28	372	0.5	50 M (50 M)	Run-21
7.7	3.85	C	0	420	90	100 M (100 M)	Run-21
7.7	31.2	FXT	2.10	420	0.5+1.0+ scattered	50 M + 112 M + 100 M (100 M)	Run-19+20+21
7.2	26.5	FXT	2.02	443	2+Parasitic with CEC	155 M + 317 M	Run-18+20
6.2	19.5	FXT	1.87	487	1.4	118 M (100 M)	Run-20
5.2	13.5	FXT	1.68	541	1.0	103 M (100 M)	Run-20
4.5	9.8	FXT	1.52	589	0.9	108 M (100 M)	Run-20
3.9	7.3	FXT	1.37	633	1.1	117 M (100 M)	Run-20
3.5	5.75	FXT	1.25	666	0.9	116 M (100 M)	Run-20
3.2	4.59	FXT	1.13	699	2.0	200 M (200 M)	Run-19
3.0	3.85	FXT	1.05	721	4.6	259 M -> 2B(100 M -> 2B)	Run-18+21



Good particle identification in a broad momentum range using TPC and TOF

STAR ☆ Hadron yields/spectra

Phys. Rev. C 96, 44904 (2017)

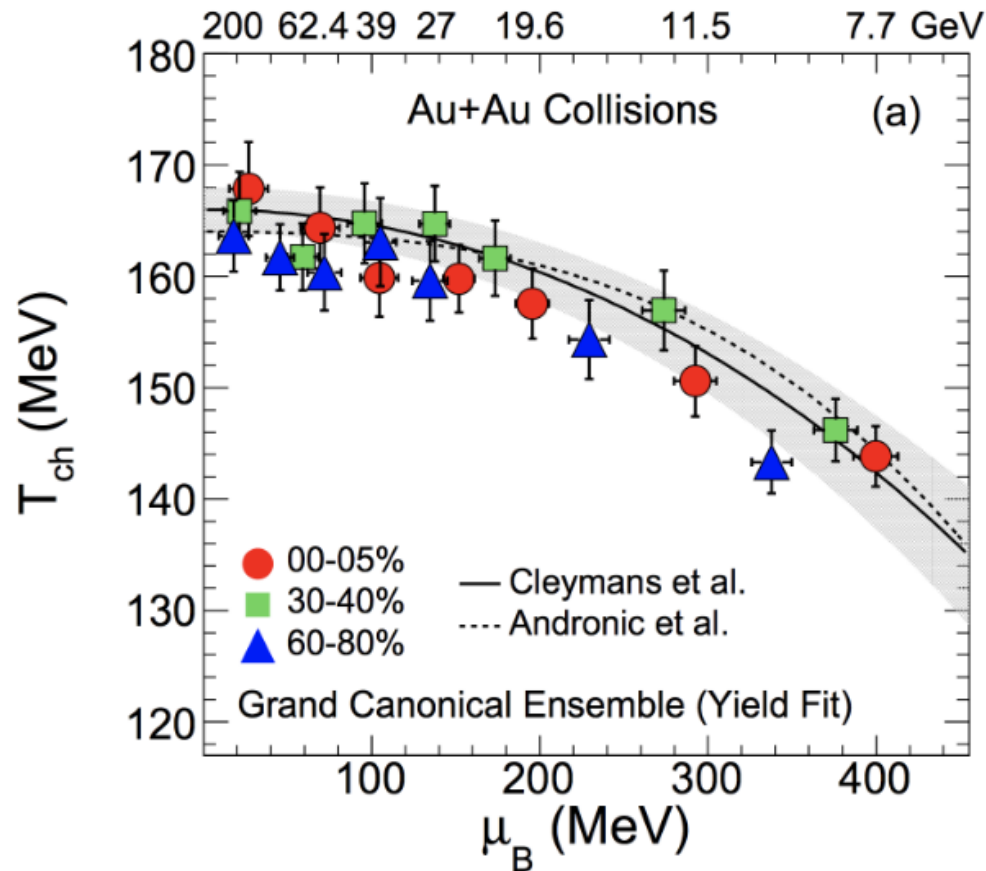


Particle ratios and p_T spectra are measured at BES, from which the freeze-out conditions can be extracted

STAR ☆ Freeze-out conditions

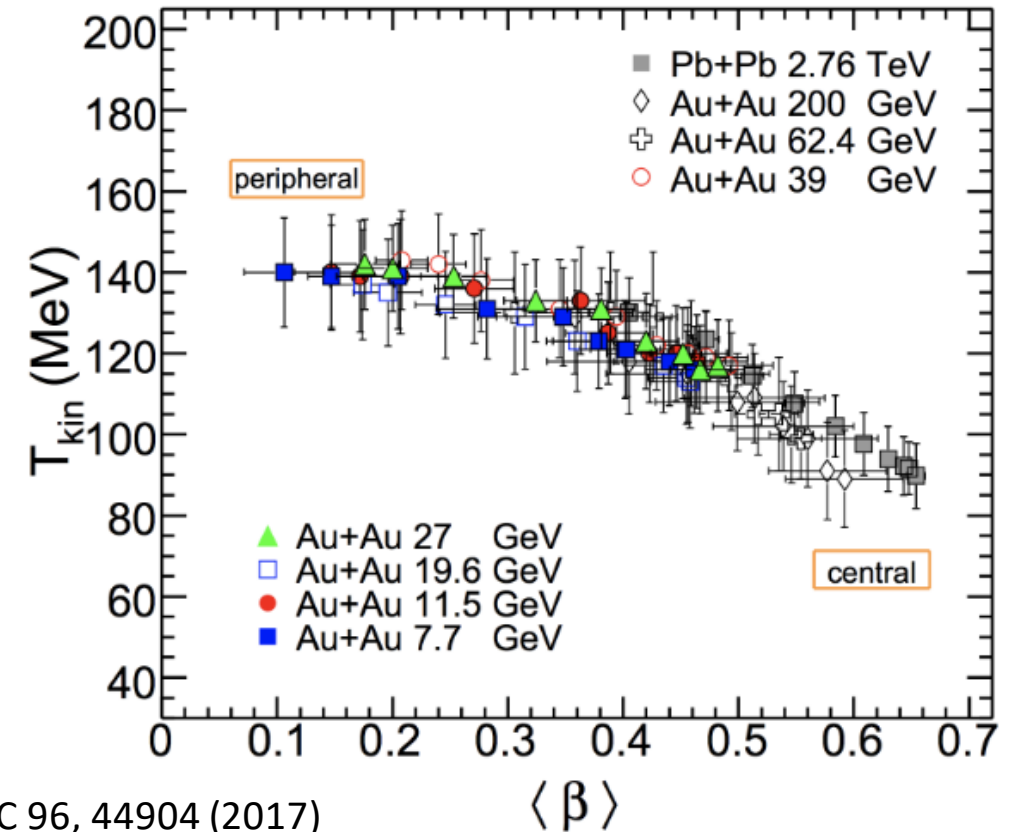
Chemical freeze-out

- Weak temperature dependence
- Centrality dependence of μ_B



Kinetic freeze-out

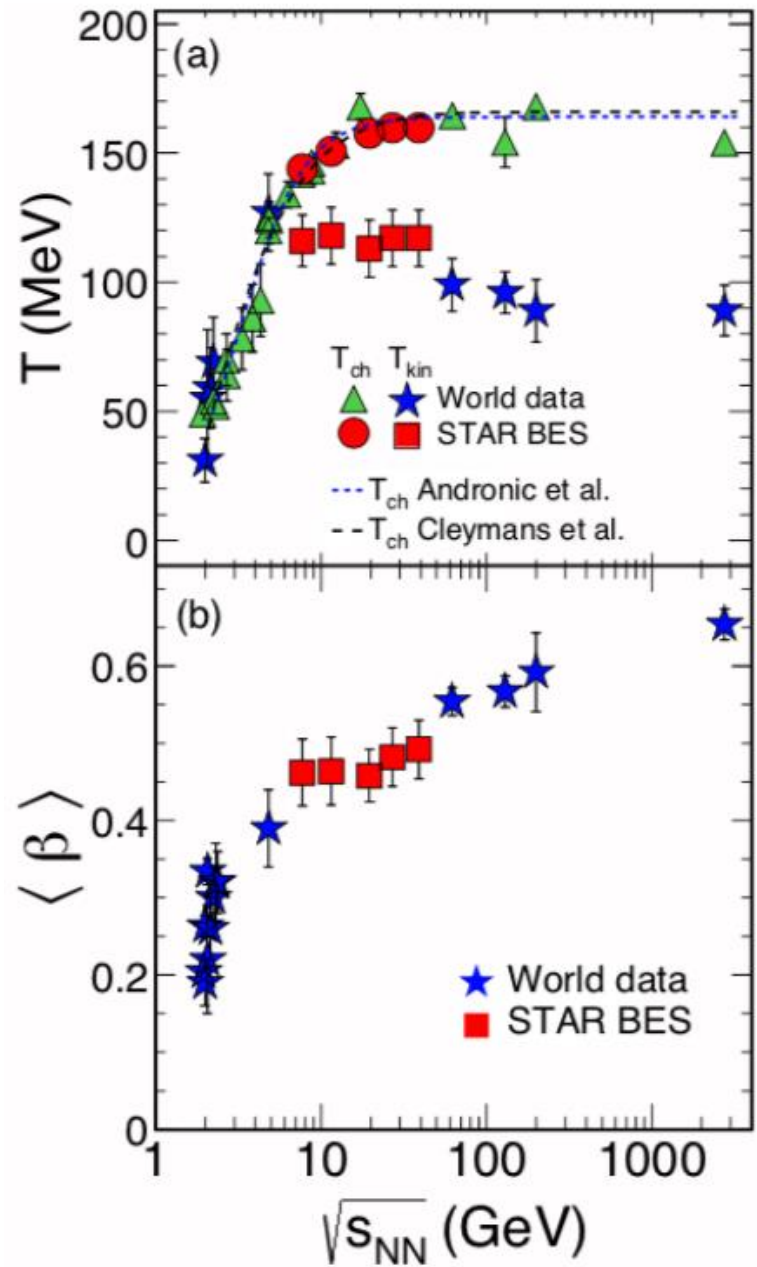
- Central collisions \rightarrow lower value of T_{kin} and larger collectivity $\langle \beta \rangle$
- Stronger collectivity at higher energy, even for peripheral collisions



Phys. Rev. C 96, 44904 (2017)

STAR Freeze-out conditions

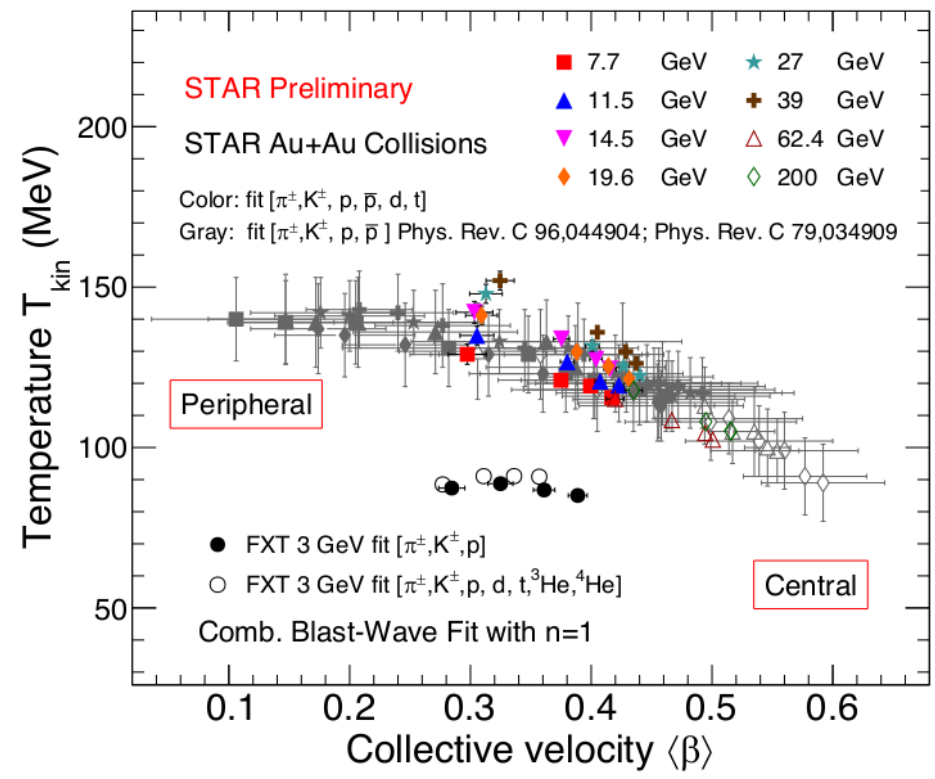
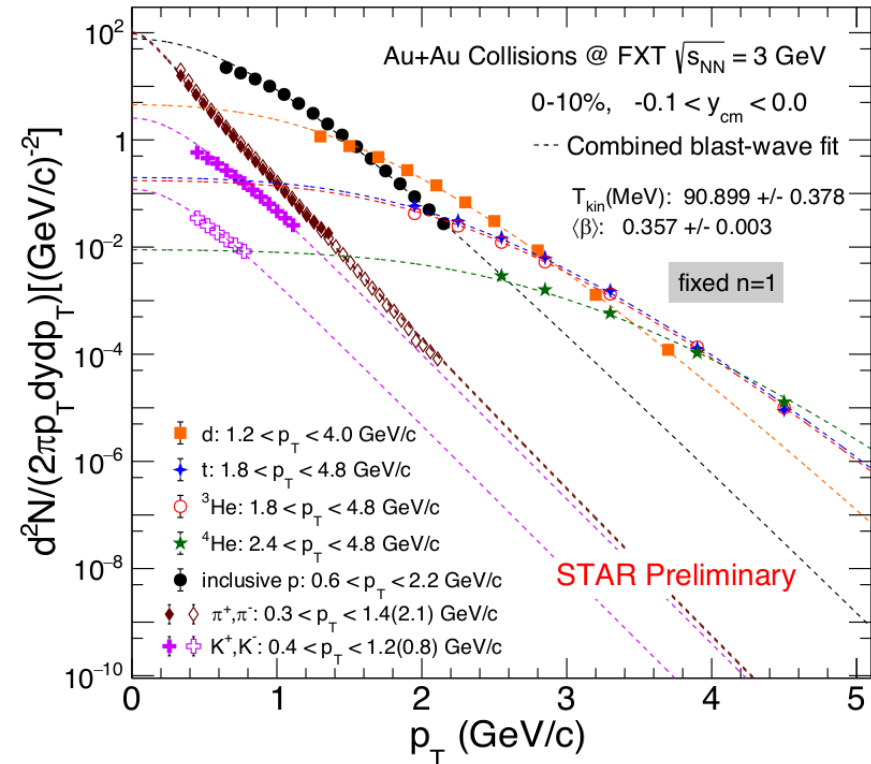
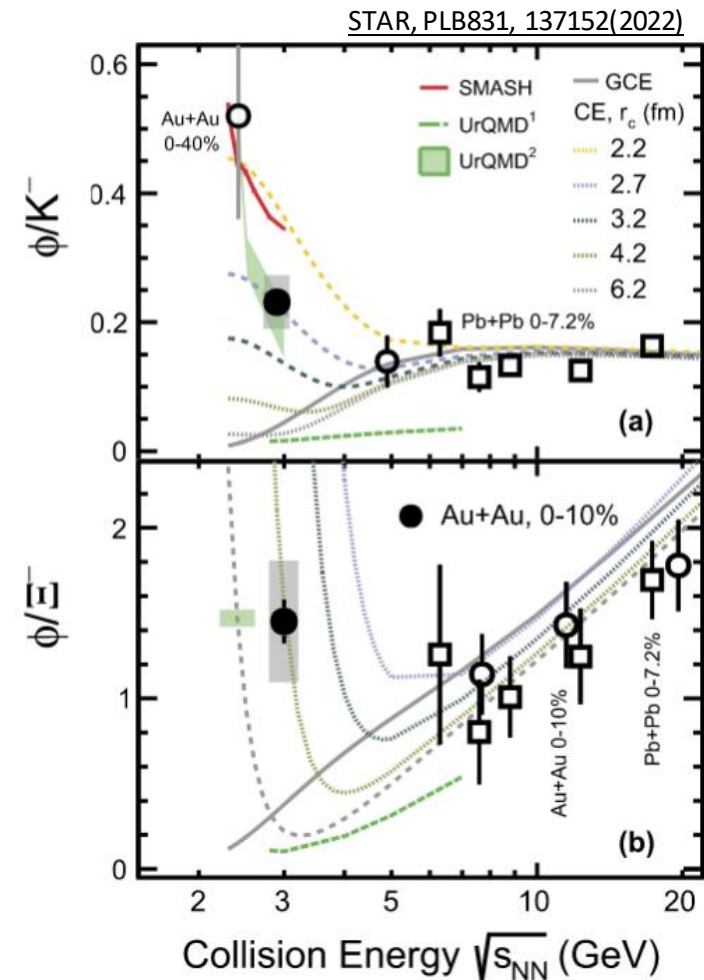
Phys. Rev. C 96, 44904 (2017)



✓ Collectivity increases with beam energy for central collisions

✓ Gap between chemical and kinetic freeze-out temperatures increases with beam energy, which suggests hadronic system interacts for longer duration in high energy collisions.

STAR ☆ Particle Production at 3 GeV



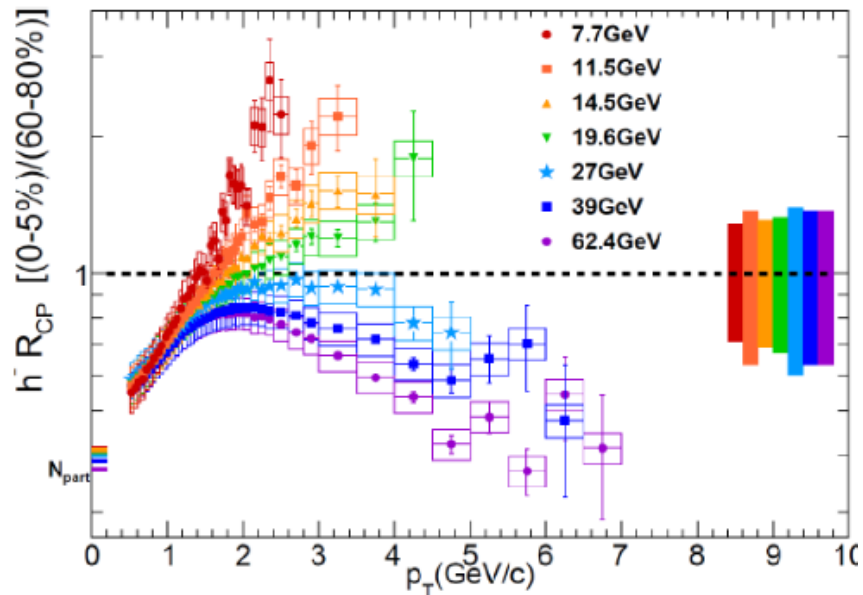
- Light nuclei p_T and rapidity distributions have been studied
- Midrapidity blast-wave fits:
 - Light nuclei prefer slightly higher T_{kin} , lower β
 - Combined fit to all particles successful

Different trend as compared to higher $\sqrt{s_{NN}}$ - different EOS at 3 GeV?

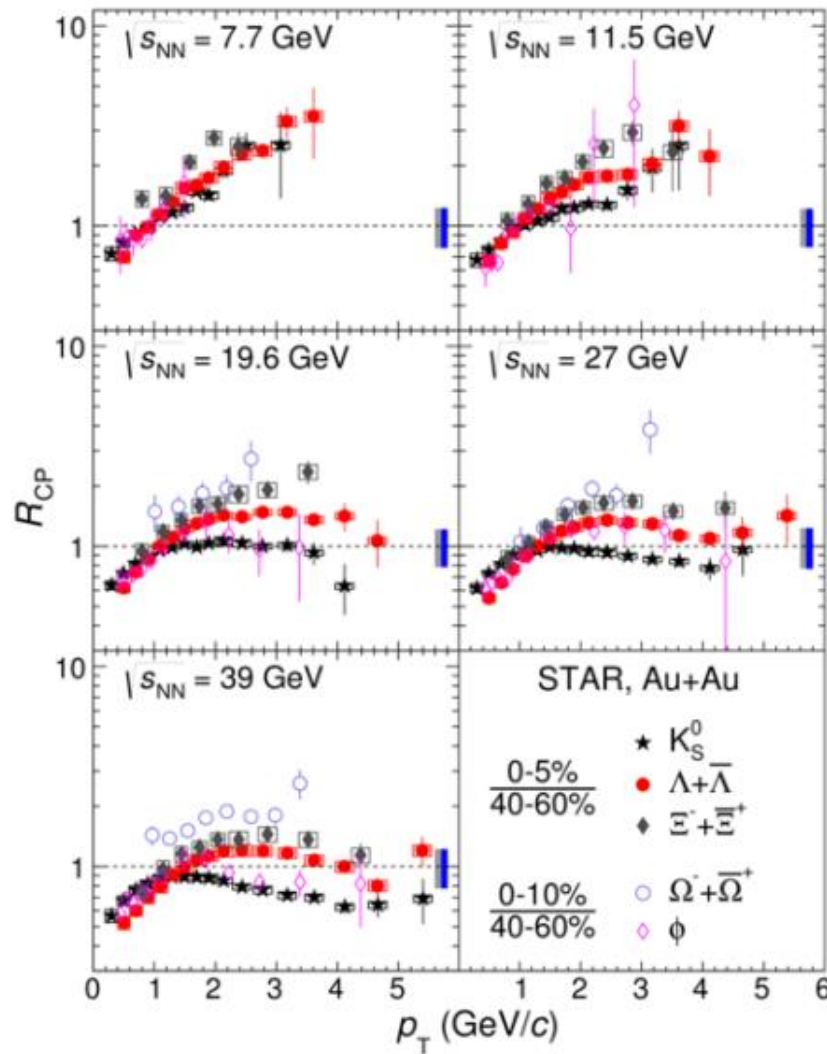
Strange particle ratios indicate the thermal particle phase space at low energies is far from the GCE limit and the local treatment of strangeness conservation is crucial

STAR ☆ Nuclear Modification in the Medium

$$R_{cp} = \frac{d^2 N dp_t d\eta / \langle N_{coll} \rangle (central)}{d^2 N dp_t d\eta / \langle N_{coll} \rangle (peripheral)}$$



Phys. Rev. C 102 (2020) 34909
Phys. Rev. Lett. 121 (2018) 32301



R_{CP} has two regimes in the behavior depending on the collision energy:

- decrease of particle production with high p_T in central collisions at high energies
- smooth growth of particle production in central collisions at low collision energies.

R_{CP} behavior changes at $\sqrt{s_{NN}} \sim 30$ GeV

High statistics of BES-II will allow to measure R_{CP} in high p_T region at low collision energies

◆ Net-baryon, net-charge and net-strangeness

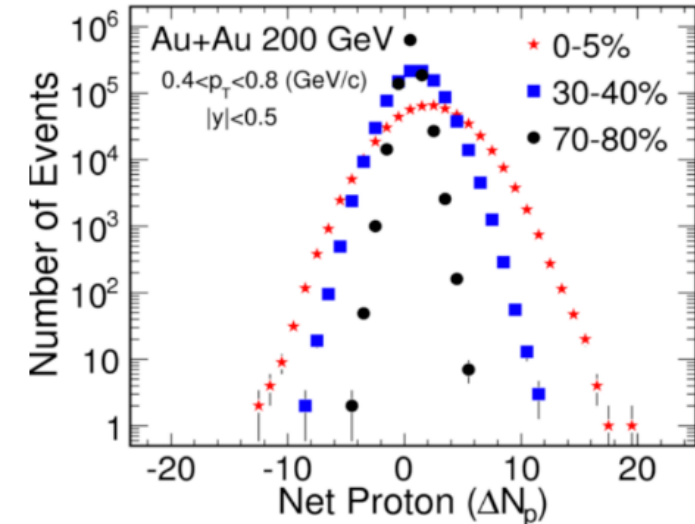
“Net” : positive - negative

$$\Delta N_q = N_q - N_{\bar{q}}, \quad q = B, Q, S$$

No. of **positively charged** particles in one collision

No. of **negatively charged** particles in one collision

Fill in histograms over many collisions



→ neutrons cannot be measured

(1) Sensitive to correlation length

$$C_2 = \langle (\delta N)^2 \rangle_c \approx \xi^2 \quad C_5 = \langle (\delta N)^5 \rangle_c \approx \xi^{9.5}$$

$$C_3 = \langle (\delta N)^3 \rangle_c \approx \xi^{4.5} \quad C_6 = \langle (\delta N)^6 \rangle_c \approx \xi^{12}$$

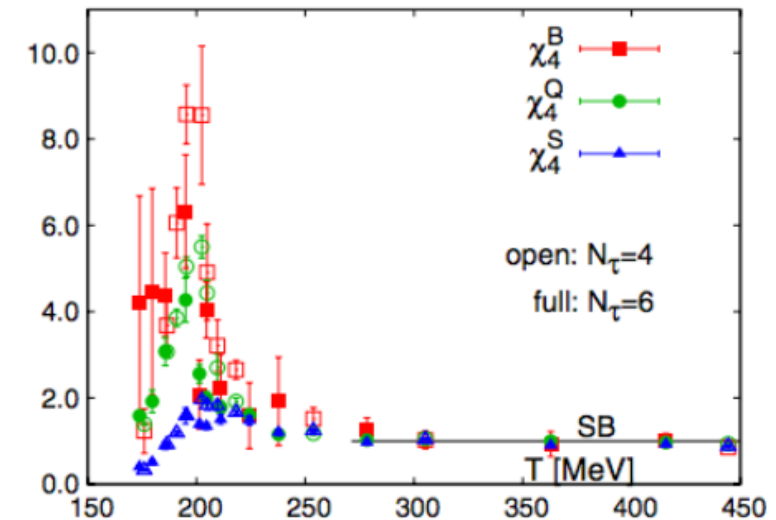
$$C_4 = \langle (\delta N)^4 \rangle_c \approx \xi^7$$

(2) Direct comparison with susceptibilities.

$$S\sigma = \frac{C_3}{C_2} = \frac{\chi_3}{\chi_2} \quad \kappa\sigma^2 = \frac{C_4}{C_2} = \frac{\chi_4}{\chi_2} \quad \frac{C_6}{C_2} = \frac{\chi_6}{\chi_2}$$

$$\chi_n^q = \frac{1}{VT^3} \times C_n^q = \frac{\partial^n p/T^4}{\partial \mu_q^n}, \quad q = B, Q, S$$

Volume dependence can be canceled by taking the ratio.



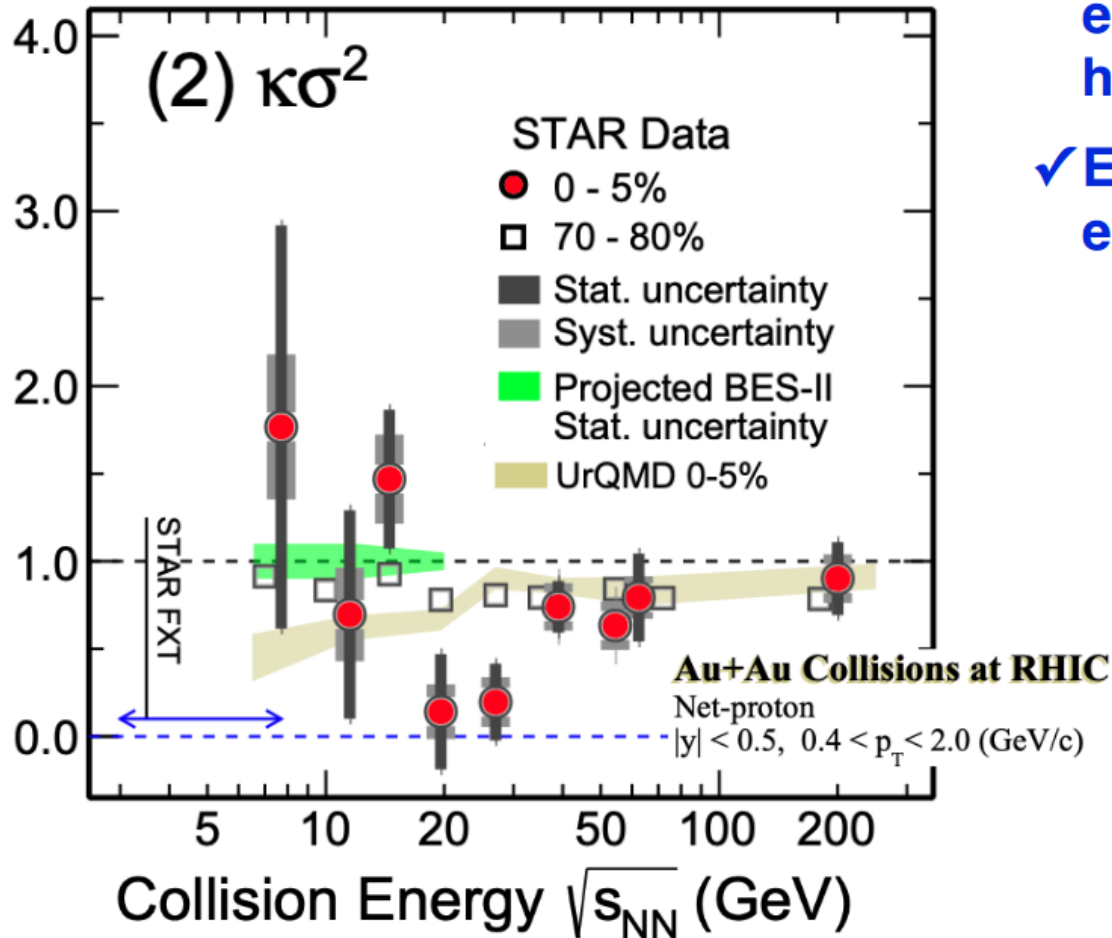
M. Cheng et al, PRD 79, 074505 (2009)

STAR ☆ Hints of Critical Fluctuations

$$\begin{aligned} \langle \delta N \rangle &= N - \langle N \rangle \\ C_1 &= M = \langle N \rangle \\ C_2 &= \sigma^2 = \langle (\delta N)^2 \rangle \\ C_3 &= S\sigma^3 = \langle (\delta N)^3 \rangle \\ C_4 &= \kappa\sigma^4 = \langle (\delta N)^4 \rangle - 3 \langle (\delta N)^2 \rangle^2 \end{aligned}$$

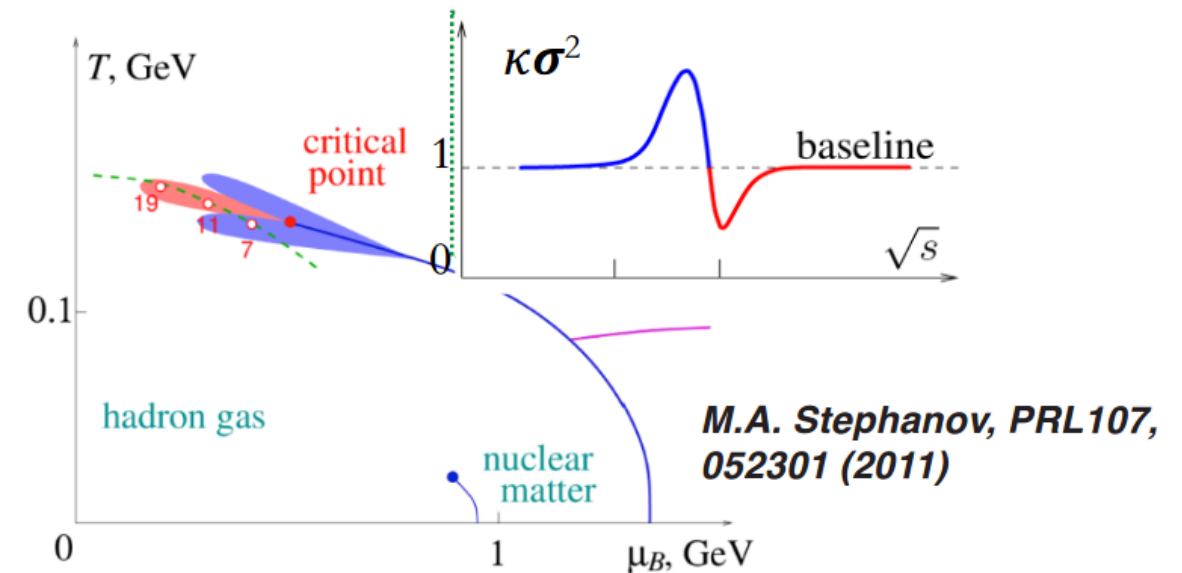
PRL 126 (2021) 92301

STAR Collaboration, PRC 104 (2021) 24902



✓ Net-proton $\kappa\sigma^2$ (C_4/C_2) shows a non-monotonic behaviour. The trend is consistent with the expectation from theoretical calculations having a critical point.

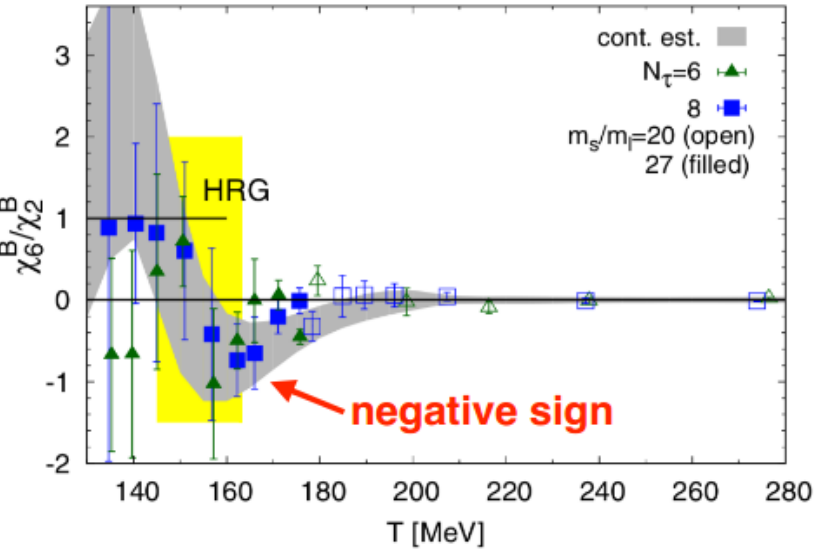
✓ Enhancement at low beam energies cannot be explained by baryon number conservation.



STAR ☆ Hints of Critical Fluctuations

- There isn't yet any direct experimental evidence for the smooth cross over at $\mu_B \sim 0$ MeV
- $C_6/C_2 < 0$ is predicted as a signature of cross over transition
- High-statistics data sets at $\sqrt{s_{NN}} = 27, 54.4, \text{ and } 200$ GeV are analyzed to look for the experimental signature of cross over transition

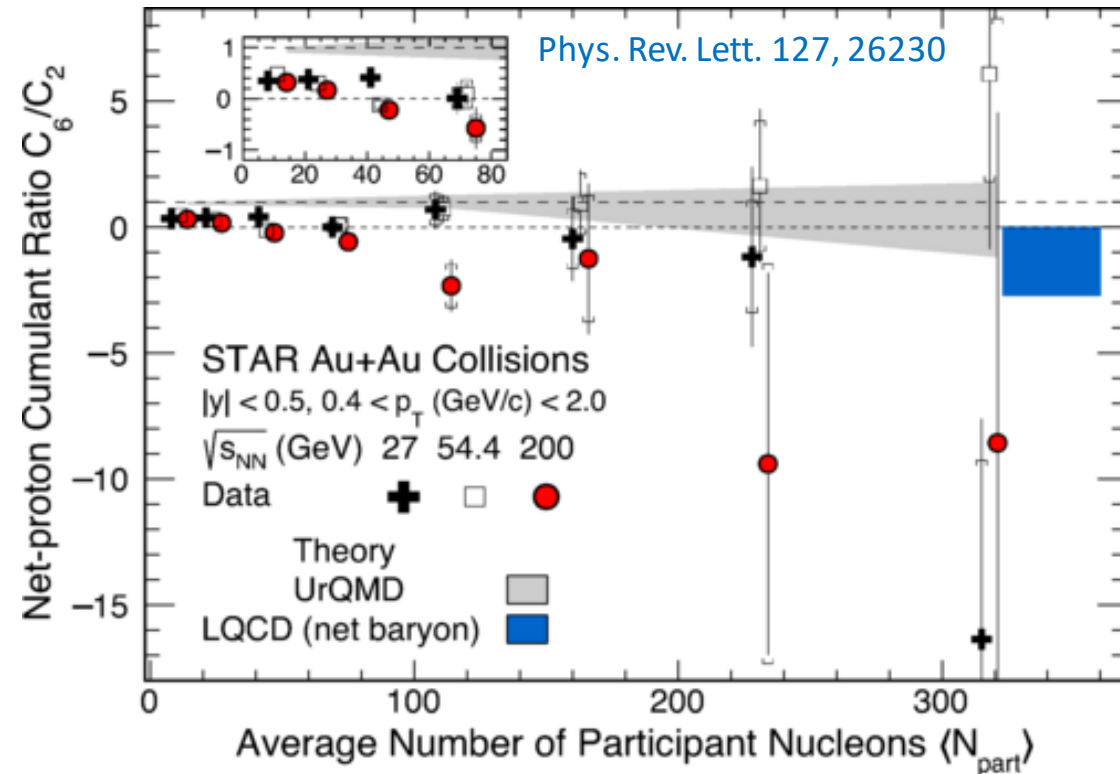
A. Bazavov et al,
PhysRevD.95.054504 : LQCD



C. Schmidt, Prog. Theor. Phys. Suppl. 186, 563–566 (2010)
 Cheng et al, Phys. Rev. D 79, 074505 (2009)
 Friman et al, Eur. Phys. J. C (2011) 71:1694

Freeze-out conditions	χ_4^B/χ_2^B	χ_6^B/χ_2^B	χ_4^Q/χ_2^Q	χ_6^Q/χ_2^Q
HRG	1	1	~ 2	~ 10
QCD: $T^{\text{freeze}}/T_{pc} \lesssim 0.9$	$\gtrsim 1$	$\gtrsim 1$	~ 2	~ 10
QCD: $T^{\text{freeze}}/T_{pc} \simeq 1$	~ 0.5	< 0	~ 1	< 0

Predicted scenario for this measurement

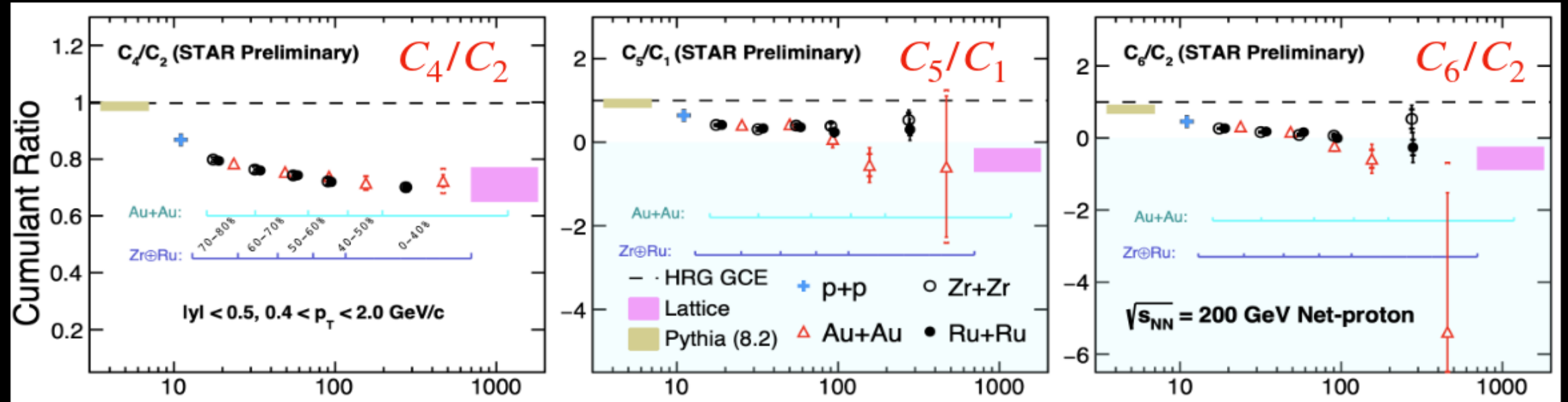


Suggestive of smooth cross over at top RHIC energies



Mapping QCD phase diagram

Multiplicity dependence of fluctuations



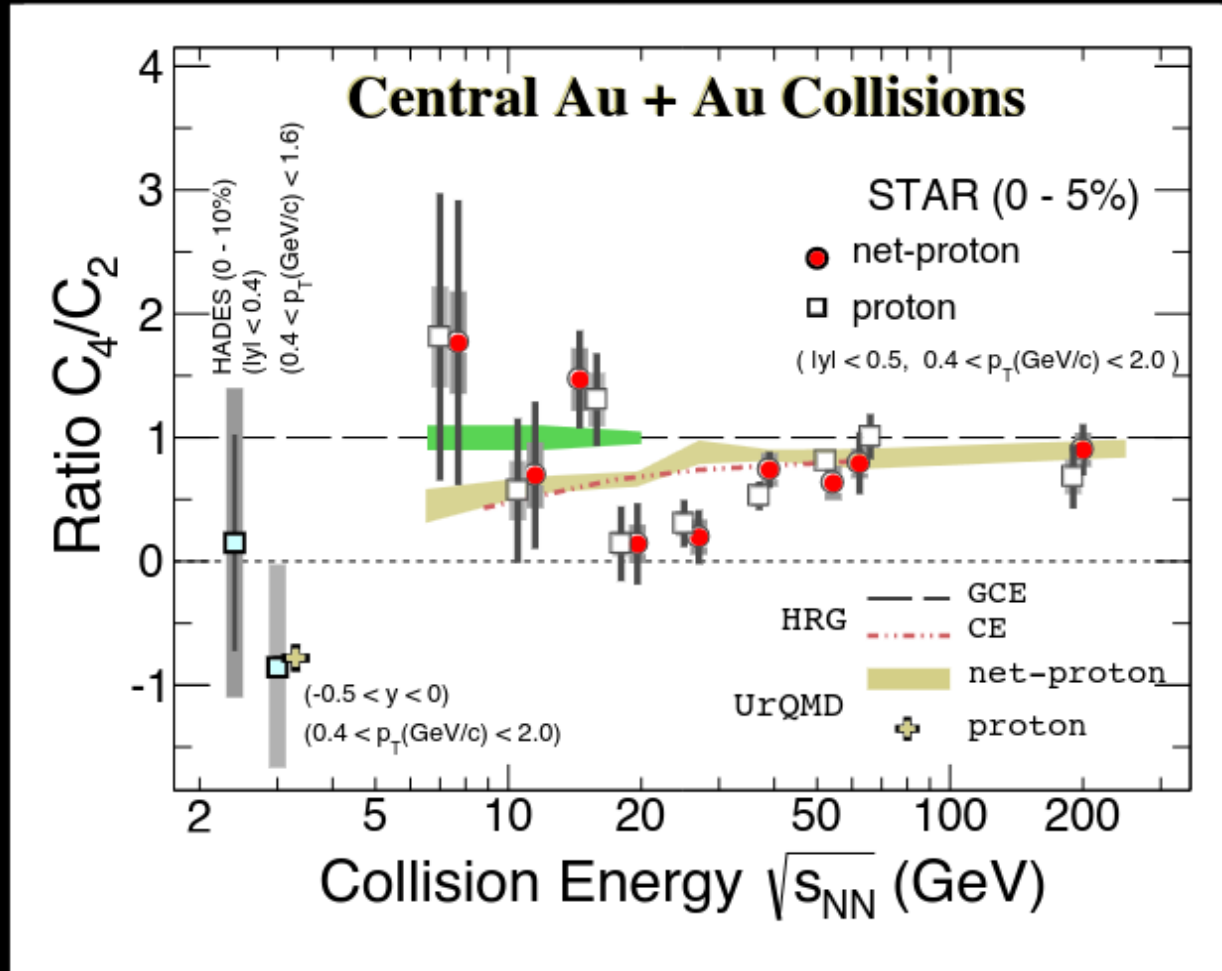
- C_4/C_2 , C_5/C_1 , and C_6/C_2 decrease with increasing multiplicity
- At high-multiplicity, cumulant ratios approach toward lattice prediction for the thermalized QCD matter and smooth crossover ($\mu_B \sim 0$)



Search for QCD critical point

Net-proton fluctuations

STAR: PRL 128, 202303 (2022)



Susceptibility

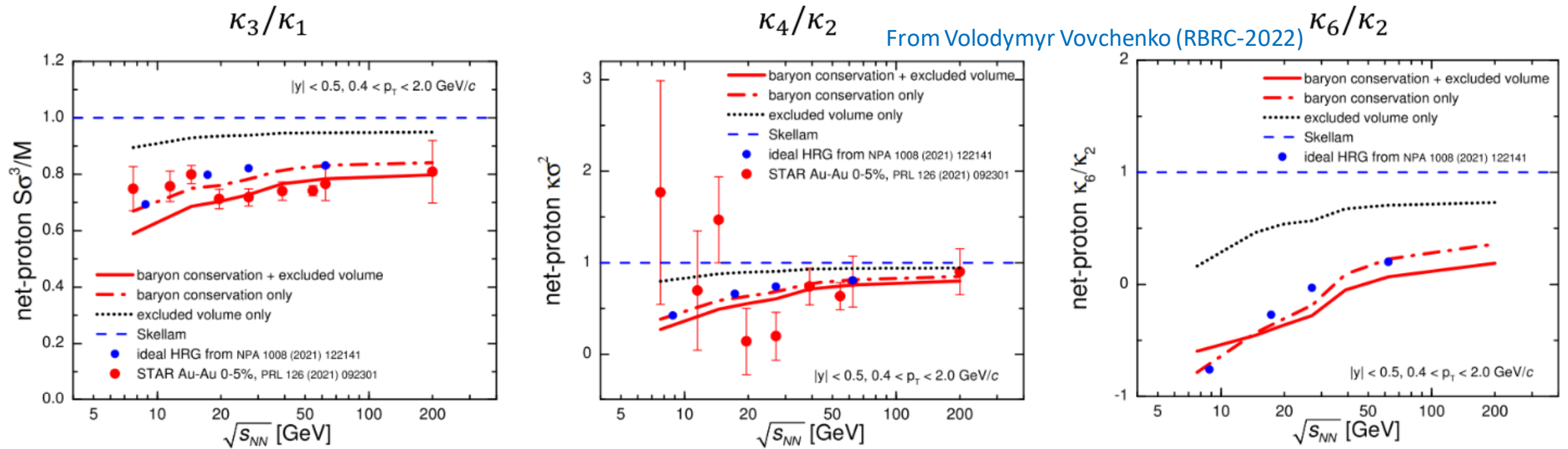
Cumulants

$$\chi_4/\chi_2 \longrightarrow C_4/C_2$$

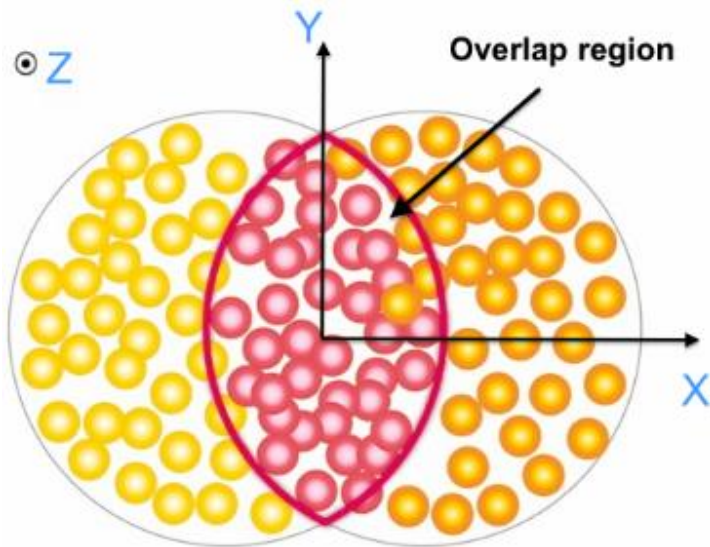
- Non-monotonic behavior as a function of $\sqrt{s_{NN}}$
Significance of 3.1σ relative to Skellam expectation

- At $\sqrt{s_{NN}} = 3$ GeV, fluctuations driven by baryon number conservation
Hadronic interaction dominates

STAR ☆ Net-proton Cumulant Ratios (theoretical calculations)



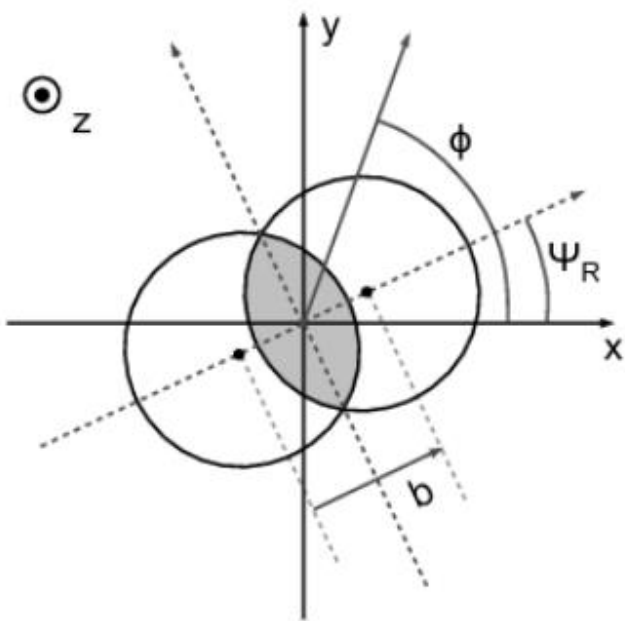
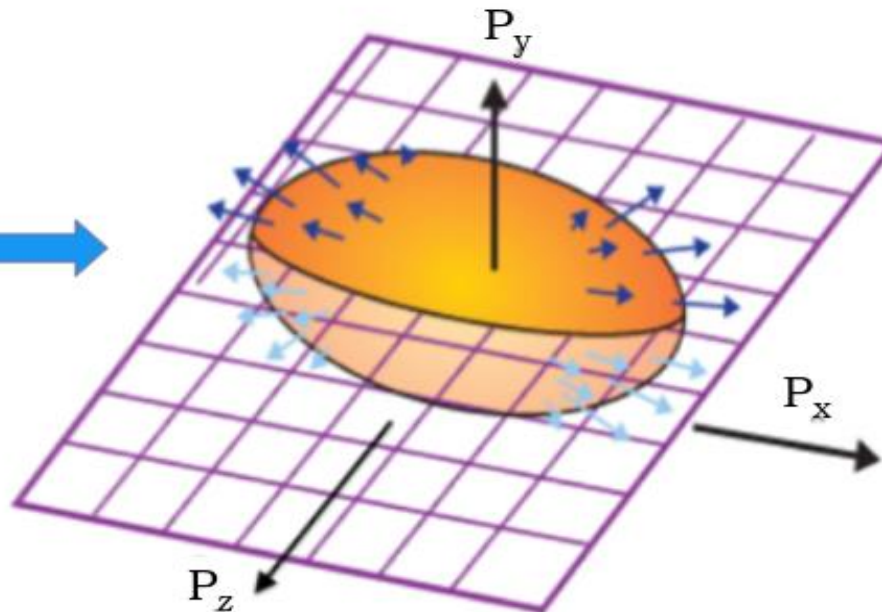
- Both the baryon conservation and repulsion needed to describe data at $\sqrt{s_{NN}} \geq 20$ GeV quantitatively
- Effect from baryon conservation is larger than from repulsion
- Canonical ideal HRG limit is consistent with the data-driven study of [Braun-Munzinger et al., NPA 1008 (2021) 122141]
- κ_6/κ_2 turns negative at $\sqrt{s_{NN}} \sim 50$ GeV



Interactions

Pressure(P)

$$y > x \rightarrow \frac{\partial P}{\partial x} > \frac{\partial P}{\partial y}$$

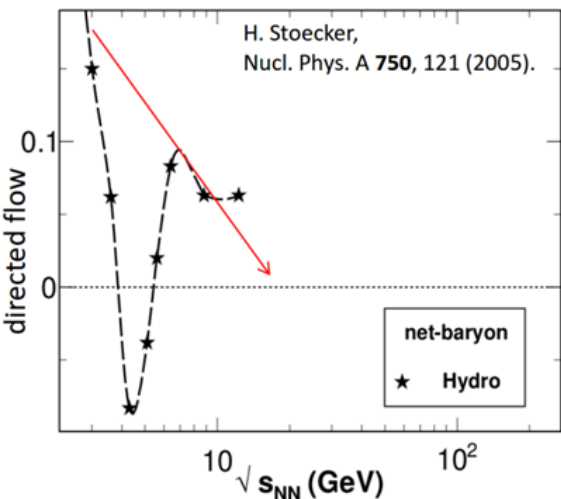


$$\frac{dN}{d\phi} \propto \frac{1}{2\pi} \left[1 + \sum_{n=1}^{\infty} 2v_n \cos(n(\phi - \psi_{rp})) \right]$$

$$v_n = \langle \cos(n(\phi - \psi_{rp})) \rangle$$

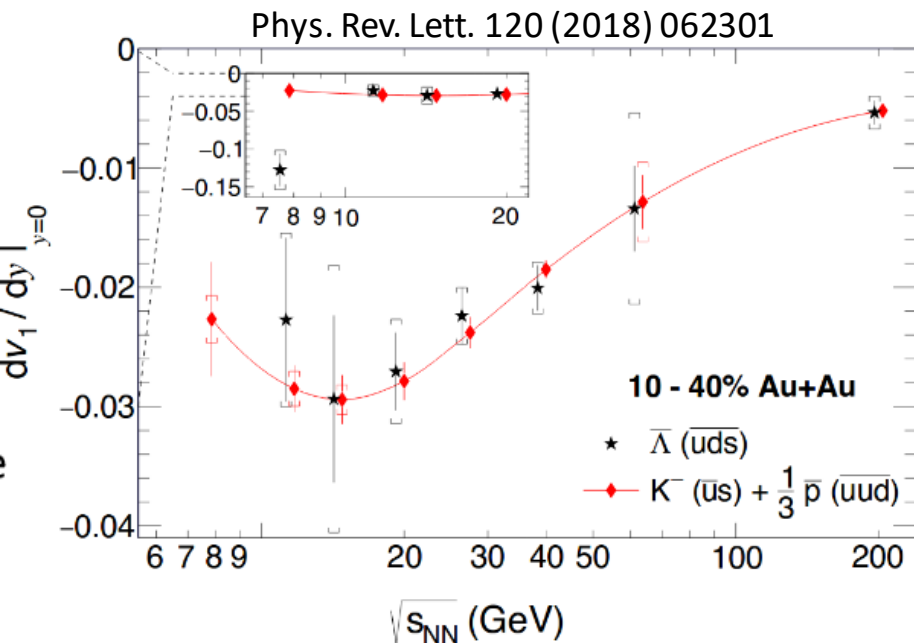
- ✓ Sensitive to early times in the evolution of the system
- ✓ Sensitive to the equation of state

Probe of the early (partonic) stage of the collision



- v_1 proposed as good probe to search for the 1st-order phase transition (strong softening)
- dv_1/dy for Λ and p agree within uncertainties
- dv_1/dy slope for baryons changes sign in the region $\sqrt{s_{NN}} < 14.5$ GeV
- Particles (anti- Λ , anti-p, and ϕ) with produced quarks show similar behavior at $\sqrt{s_{NN}} > 14.5$ GeV
- Mesons show negative dv_1/dy

Minimum in dv_1/dy slope at $\sqrt{s_{NN}} \sim 15$ GeV

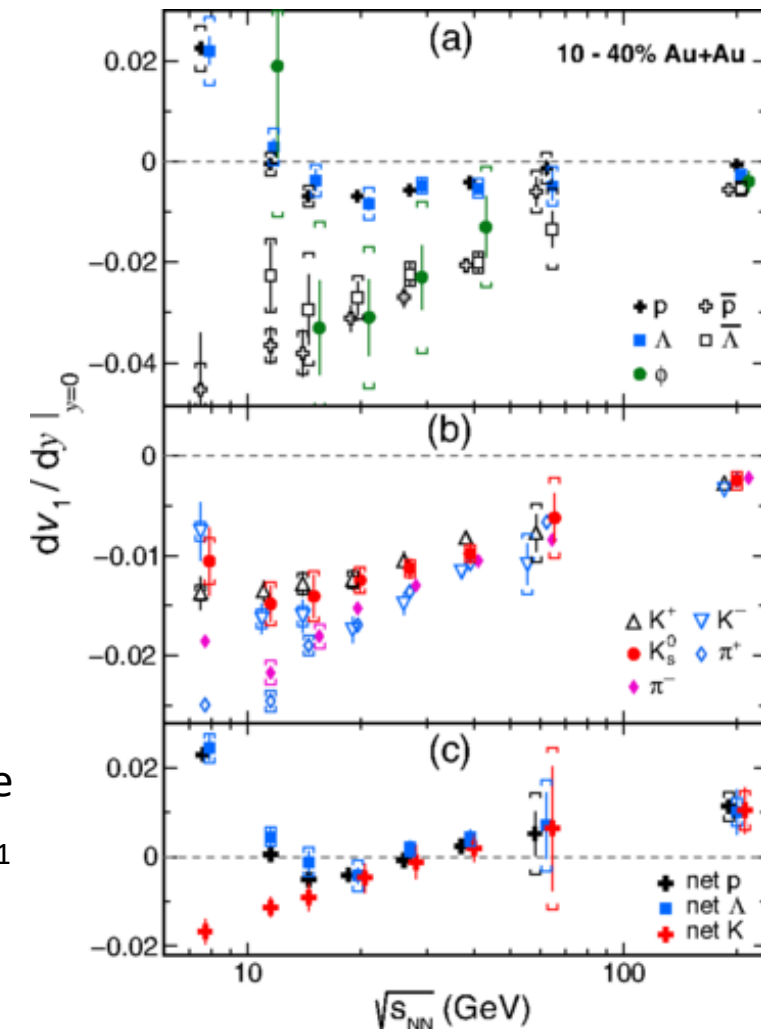


Assumption for the coalescence sum rule:

- v_1 is developed at the prehadronic stage
- Specific type of quarks have the same v_1
- Hadrons are formed via coalescence

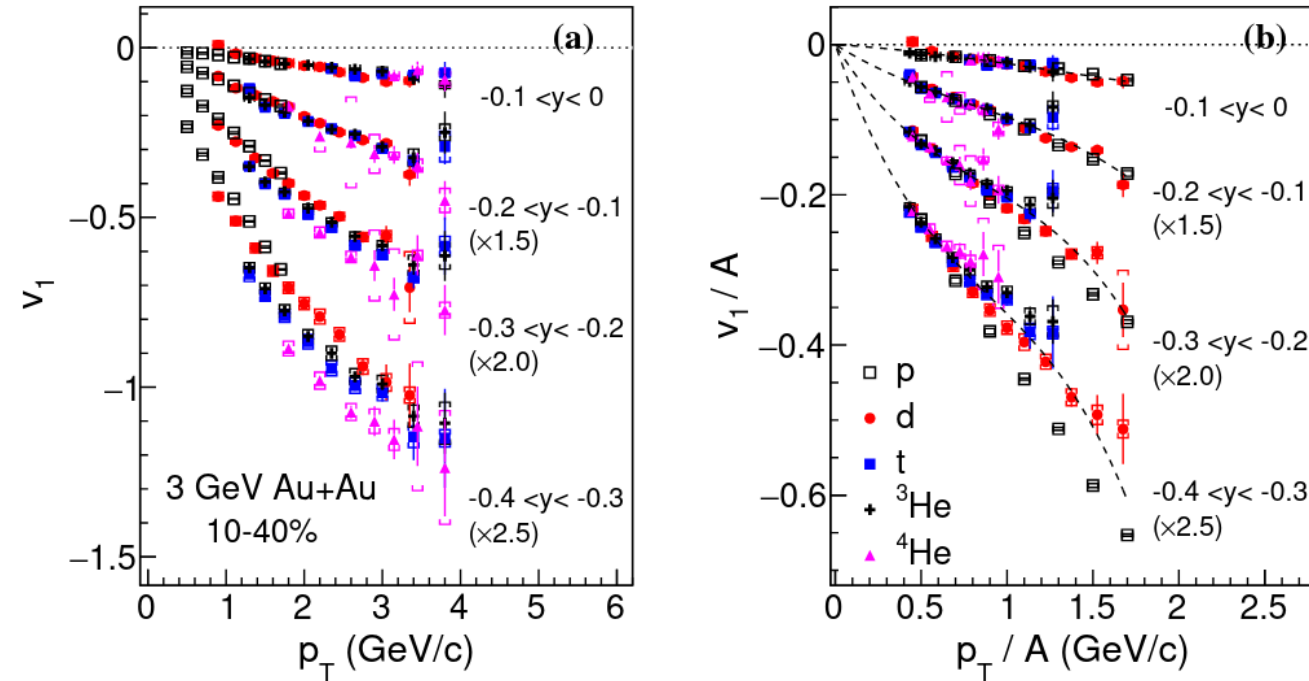
$$(v_n)_{hadron} = \sum (v_n)_{constituent\ quarks}$$

For anti-Lambda, prediction using coalescence sum rule agrees with measured v_1 above $\sqrt{s_{NN}} = 11.5$ GeV

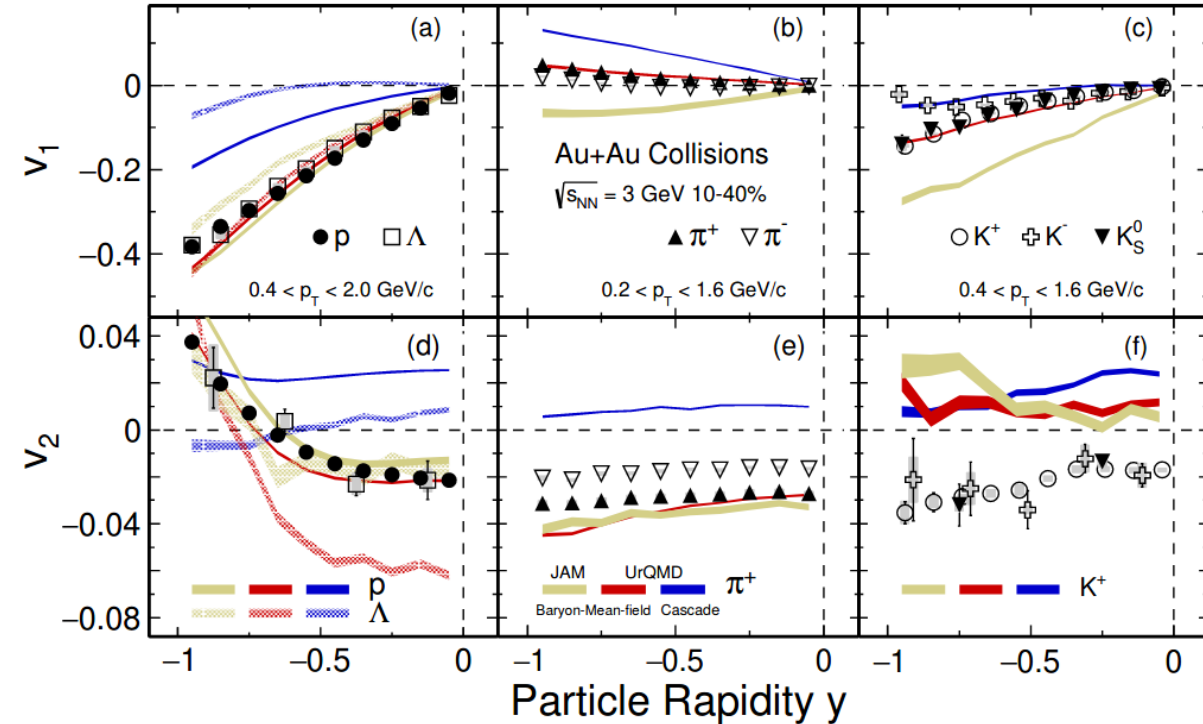


STAR Directed and Elliptic Flow

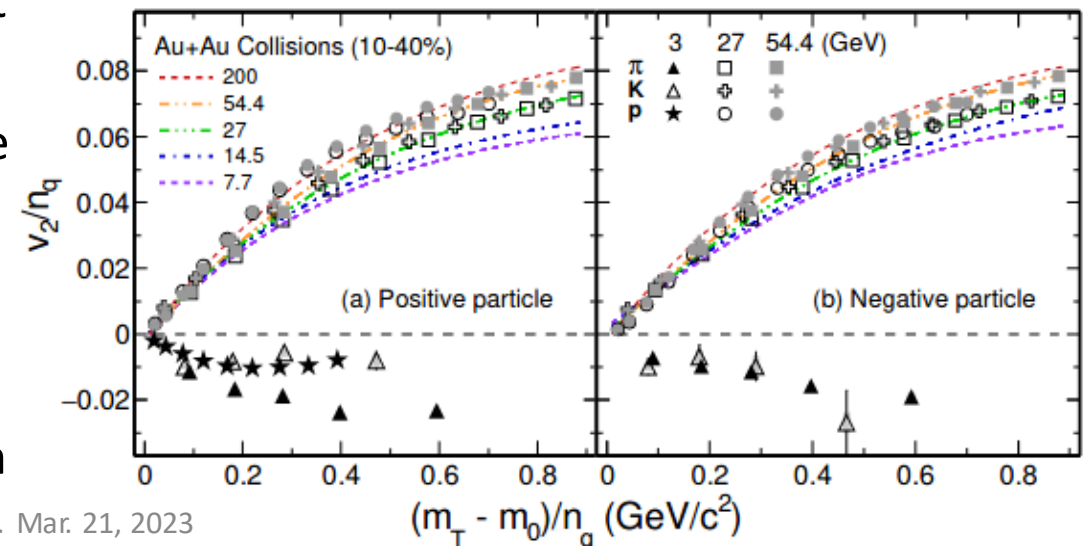
Phys. Lett. B 827 (2022) 136941



Phys. Lett. B 827 (2022) 137003



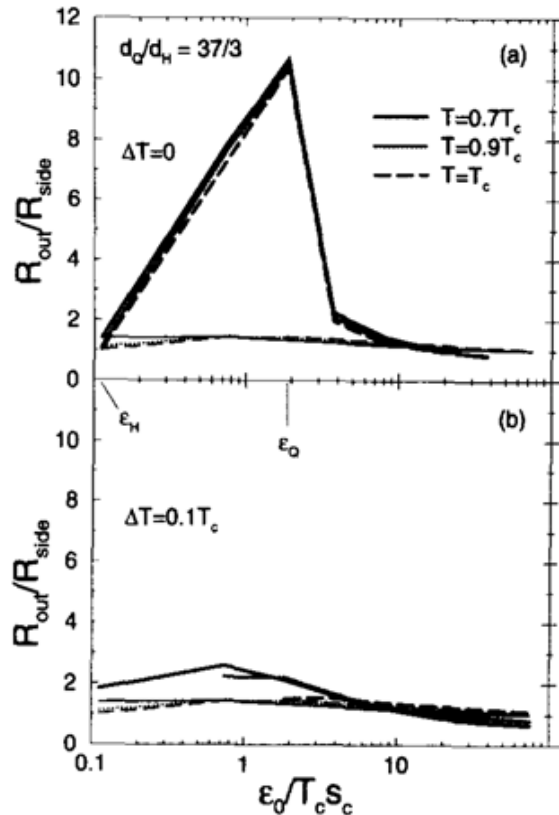
- Light nucleus $v_1(p_T)$ follows atomic-mass-number (A) scaling at different rapidity bins
- At 3 GeV, the NCQ scaling is absent and the opposite collective behavior is observed: the elliptic flow of all hadrons at midrapidity is negative; the slope of the directed flow of all hadrons, except π^+ , at midrapidity is positive.
- Observations imply the vanishing of partonic collectivity and a new EOS, likely dominated by baryonic interactions in the high baryon density region



STAR ☆ Femtoscopic correlations

- Time delays of the particle emission could be observed using femtoscopy technique (via R_{out}/R_{side} or $R_{out}^2 - R_{side}^2$) and used to search for the 1st-order phase transition

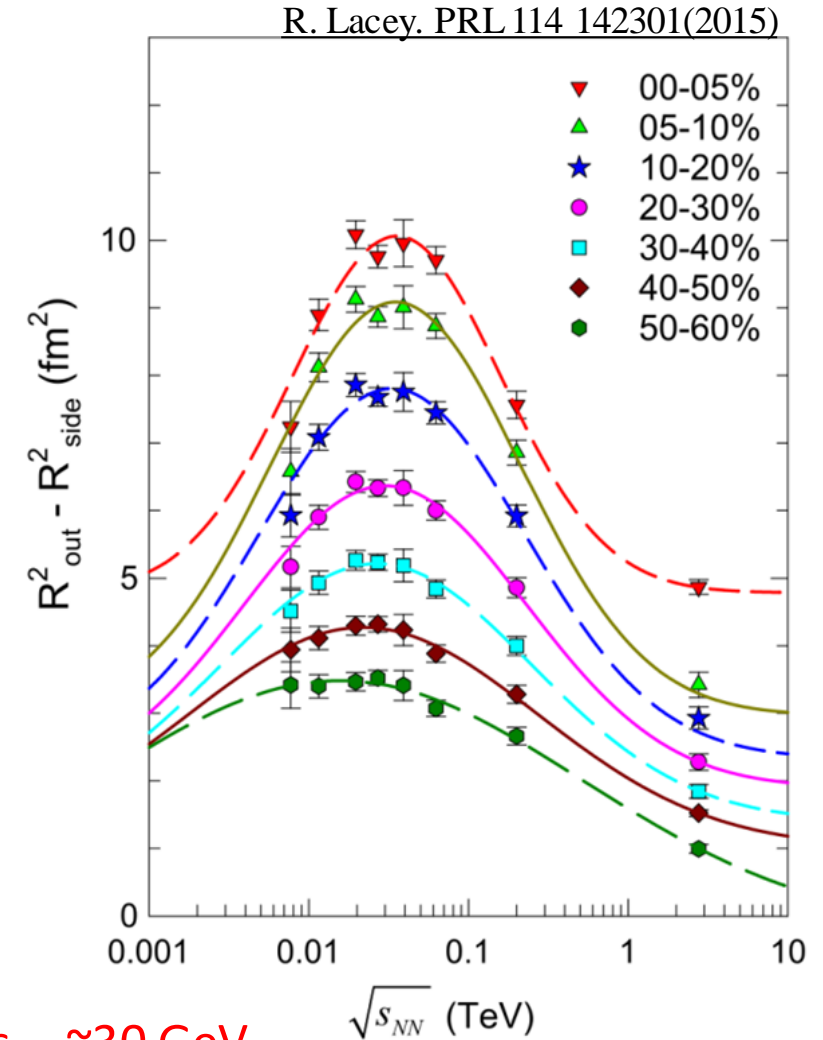
D.H. Rischke, M. Gyulassy. NPA 608 (1996) 479



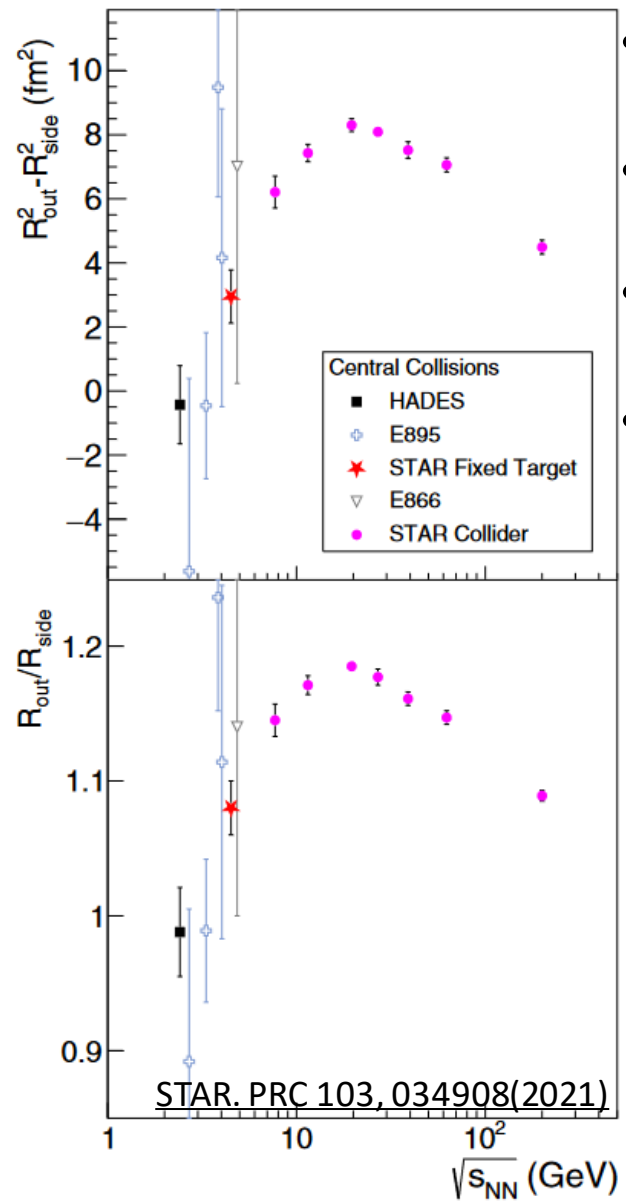
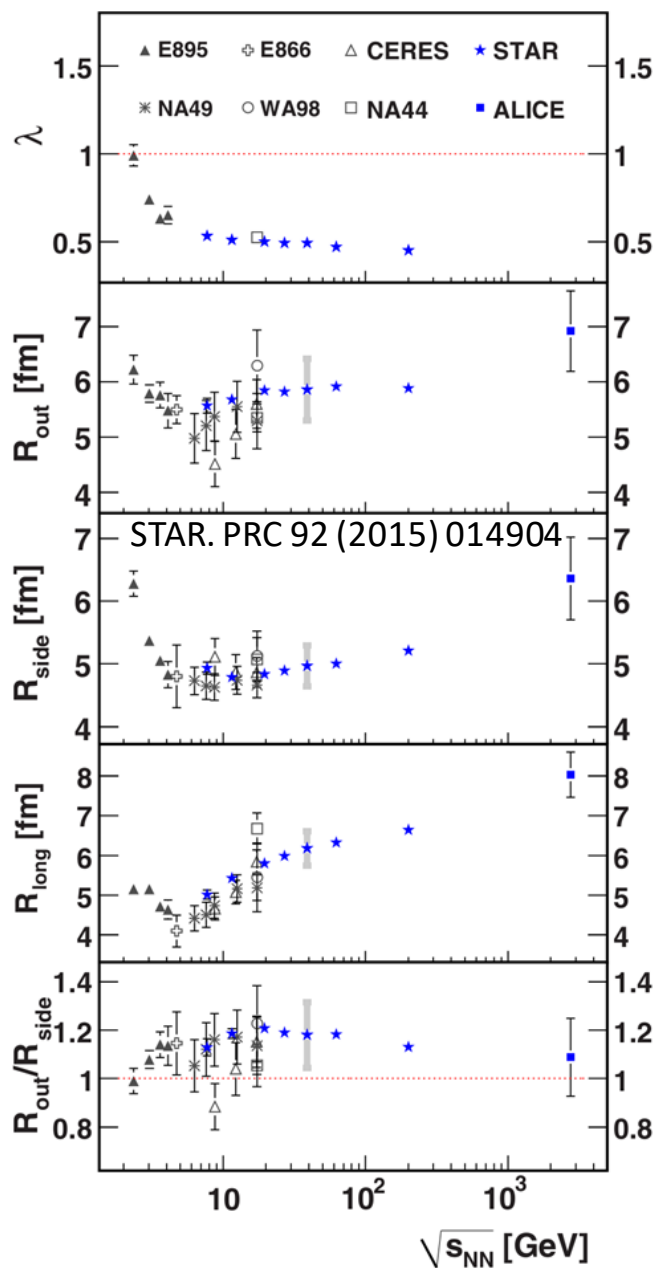
R_{side} – geometrical size

R_{out} – sensitive to geometrical size and particle emission duration

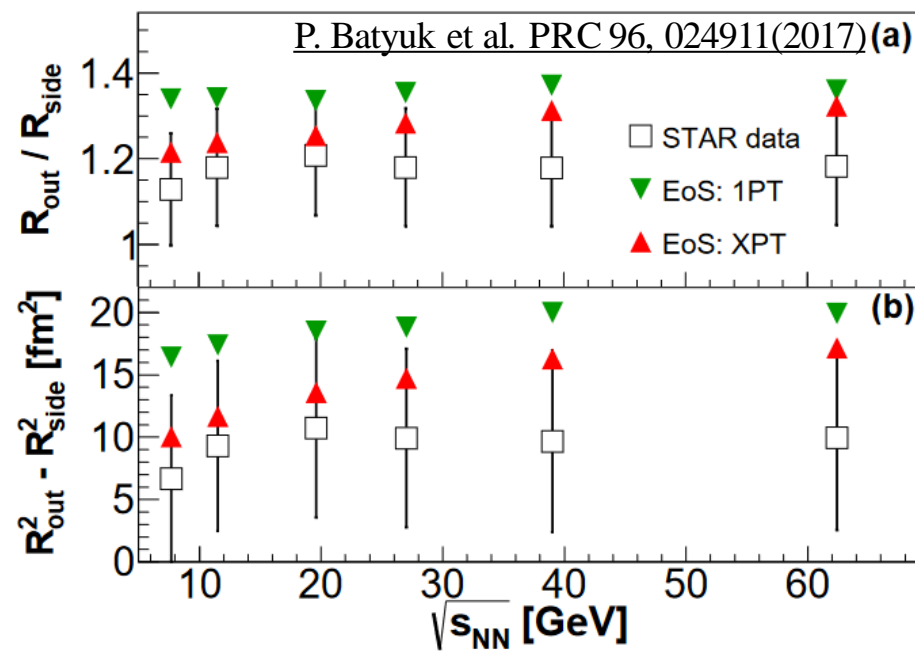
R_{long} – sensitive to the time of maximum emission



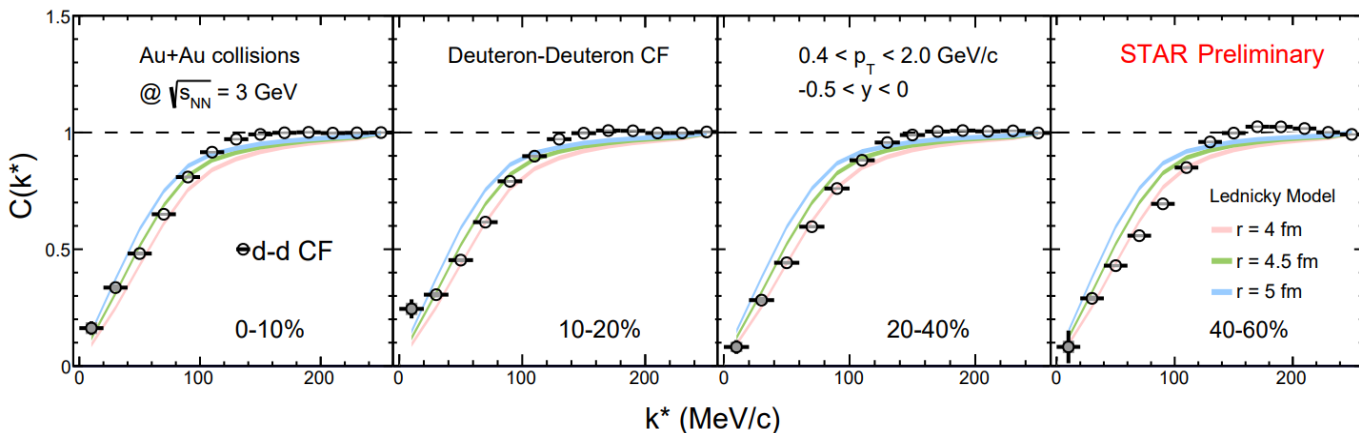
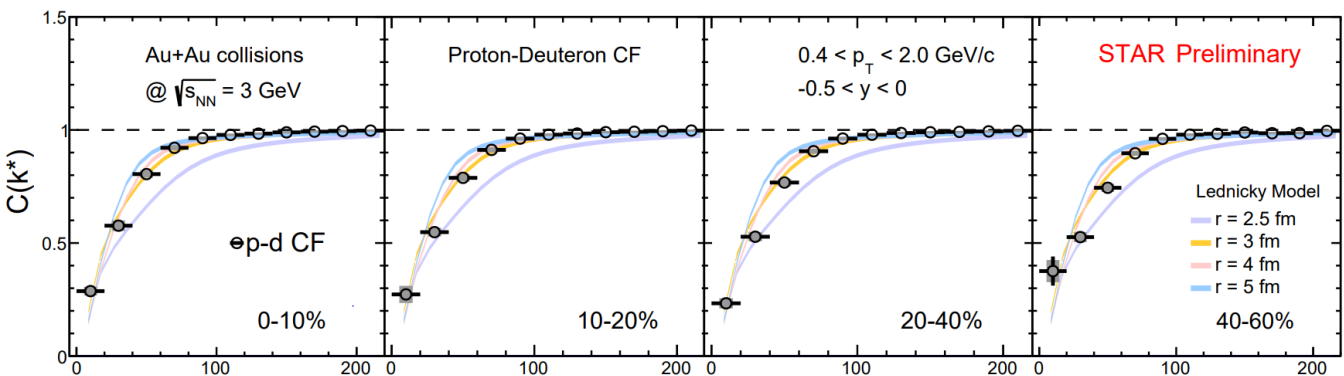
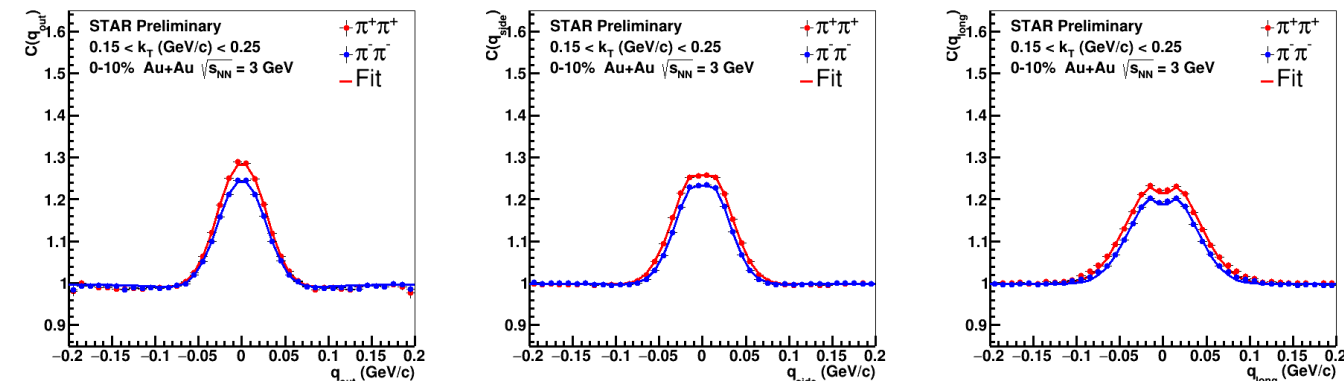
Peak structure with maximum at $\sqrt{s_{NN}} \sim 30$ GeV



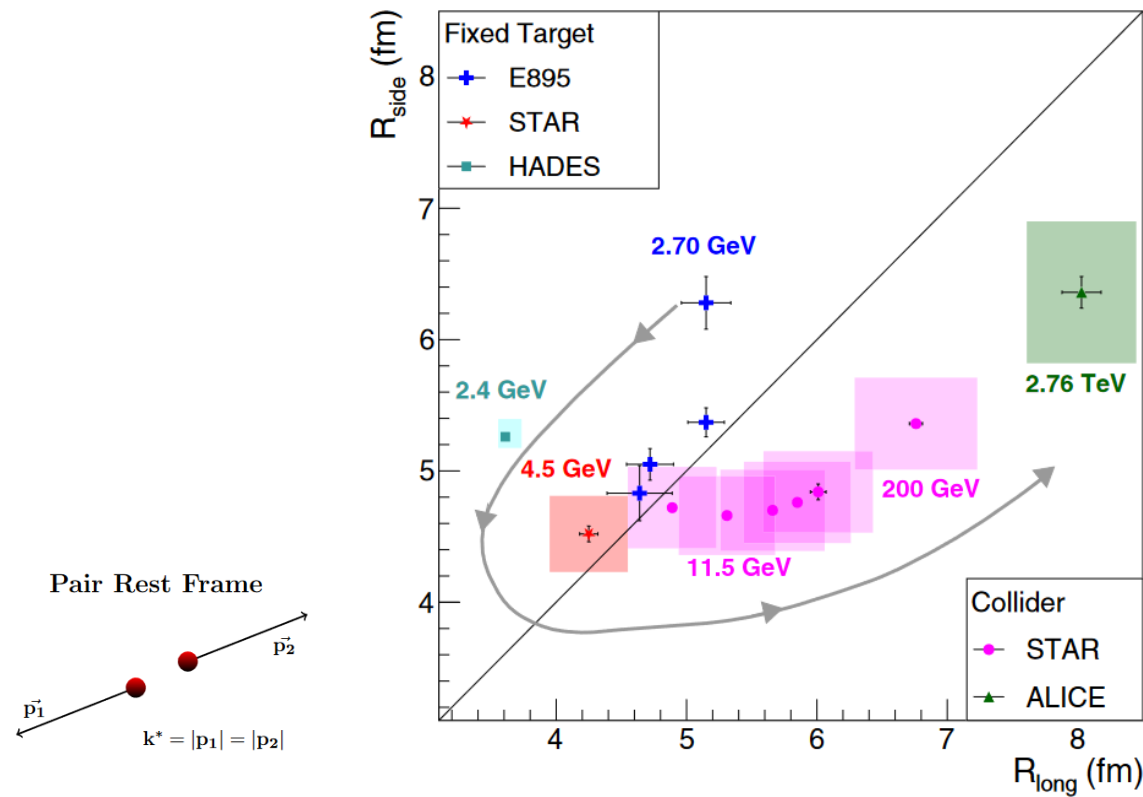
- Precise measurements in a broad energy range (from 2.41 GeV to 2.76 TeV)
- Can be reasonably described with hybrid models (initial conditions+ hydrodynamics+ hadron cascade)
- Need more high-statistics measurements at low energies
- Results can be described with hybrid models; preference to the cross over phase transition



- Many interesting results from low-energy nuclear collisions: $\pi\pi$, pp , pd , dd , and others
- Provide information about particle interactions
- The source shape evolves from oblate to prolate, as energy increases

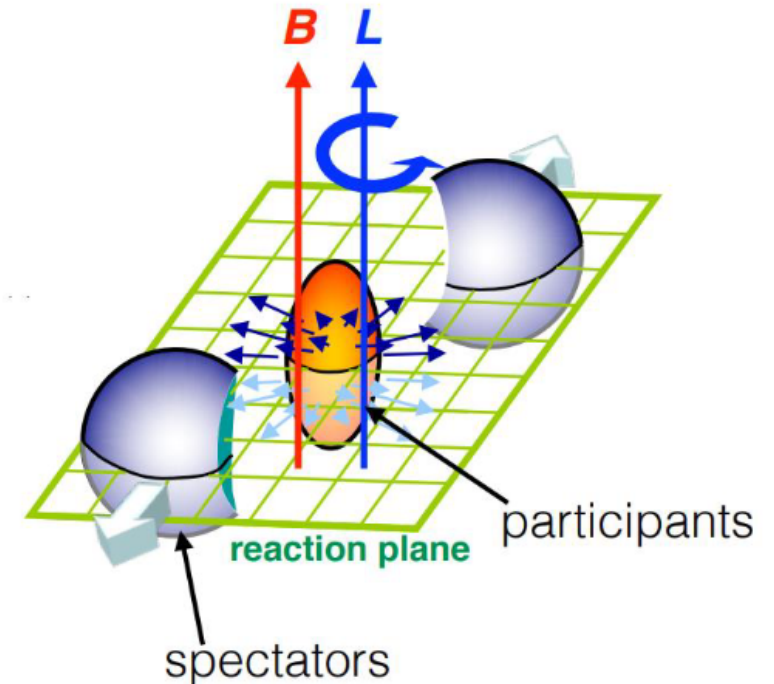


STAR. PRC 103, 034908(2021)



STAR ☆ Global hyperon polarization

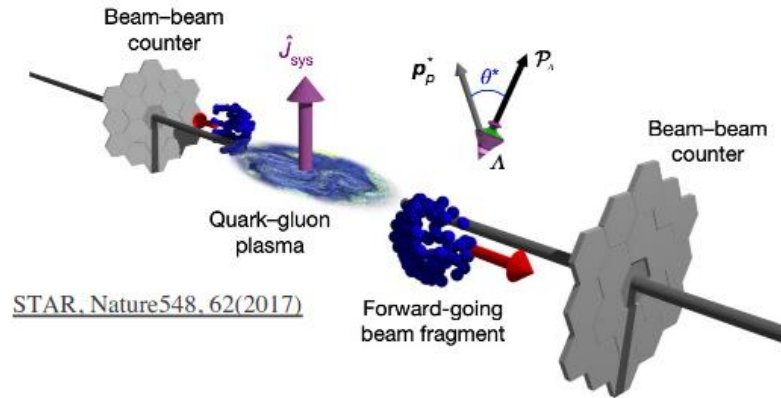
- The Quark-Gluon Plasma (QGP) formed in non-central nucleus-nucleus collisions is associated with large angular momentum, that leads to vorticity in the medium
- Spin-orbit coupling aligns spin directions of produced particles with the direction of vorticity
 - Z.-T. Liang and X.-N. Wang, PRL94, 102301 (2005)
 - S. A. Voloshin, arXiv:nucl-th/0410089
- Another possible source of particle polarization is magnetic field, created in non-central collisions in the initial stage
 - D. Kharzeev, L. McLerran, and H. Warringa, Nucl.Phys.A803, 227 (2008)
 - McLerran and Skokov, Nucl. Phys. A929, 184 (2014)



STAR ☆ Global Polarization in BES and FXT

Phys. Rev. C 104 (2021) 061901

The average vorticity points along the direction of the angular momentum of the \hat{J}_{sys}



Global polarization is measured from the angular distributions of hyperon decay product:

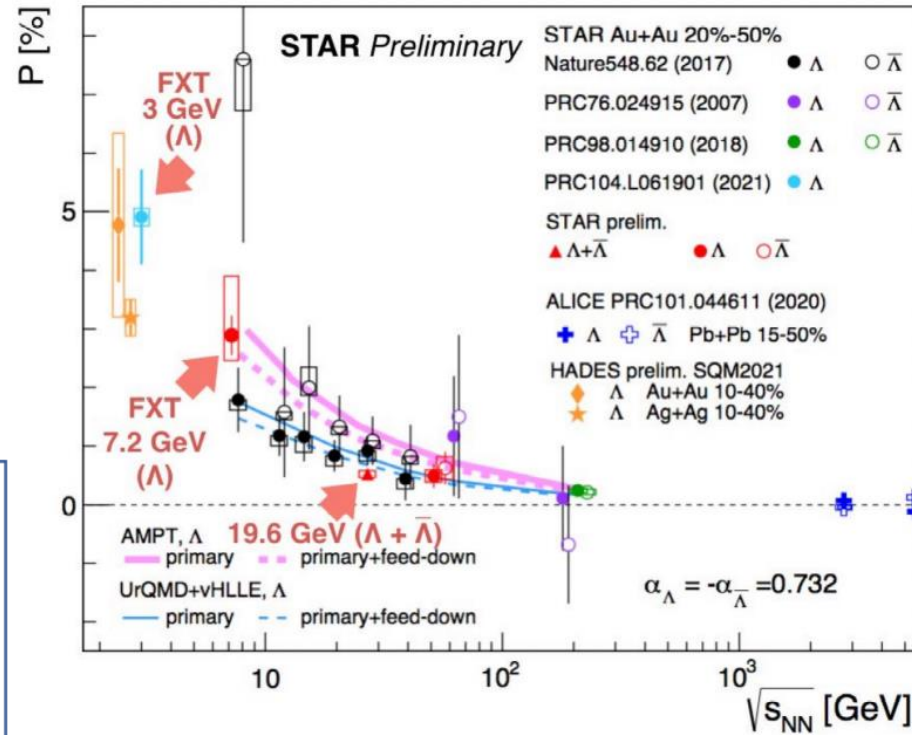
$$P_H = \frac{8}{\pi\alpha_H} \frac{\langle \sin(\Psi_1 - \phi_d^*) \rangle}{\text{Res}(\Psi_1)}$$

Thermal vorticity:

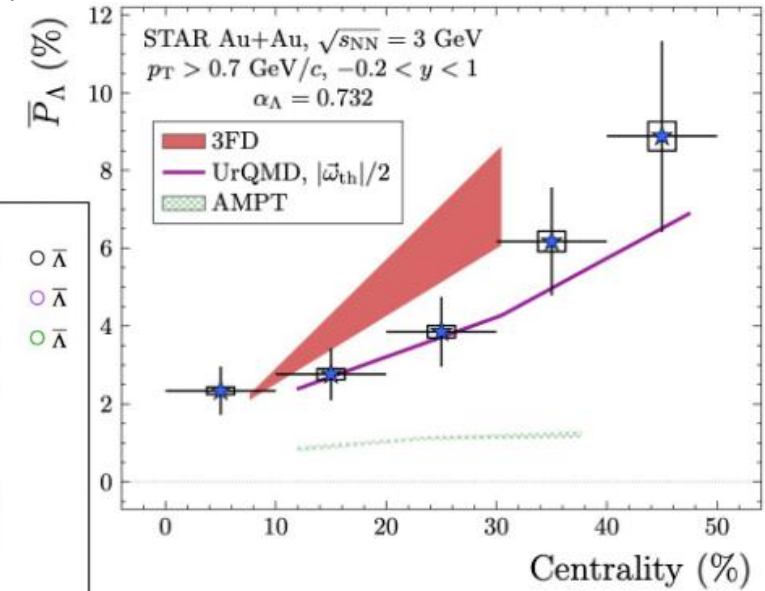
$$\omega = k_B T (P_\Lambda + P_{\bar{\Lambda}}) / \hbar \quad \omega \sim (9 \pm 1) \times 10^{21} \text{ s}^{-1}$$

F. Becattini et al., PRC95, 054902(2017)

Opens up new directions in the study of the hottest, least viscous and most vortical fluid matter.



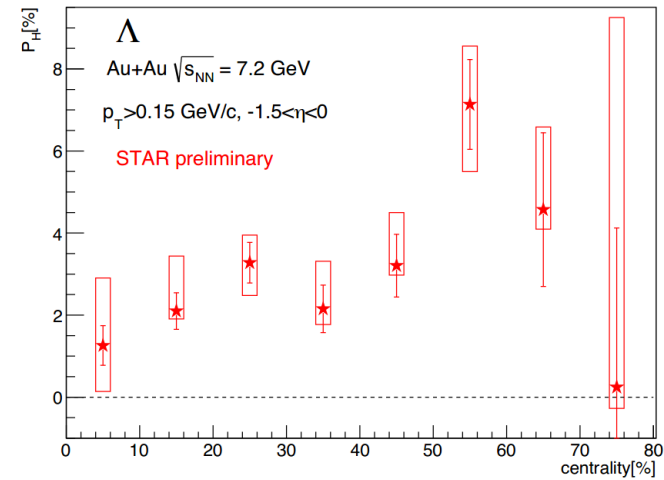
Nature 548 (2017) 62,
PRC 104 (2021) 061901,
arXiv: 2204.02302



Much larger \bar{P}_Λ in FXT 3 GeV at 20-50%

$$4.91 \pm 0.81 \text{ (stat.)} \pm 0.15 \text{ (syst.)} \%$$

Larger hyperon polarization for more peripheral collisions

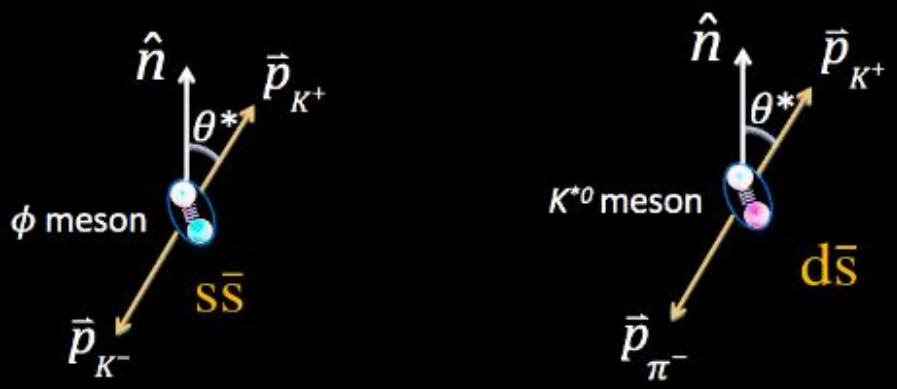




Global spin alignment of vector-mesons in heavy-ion collisions

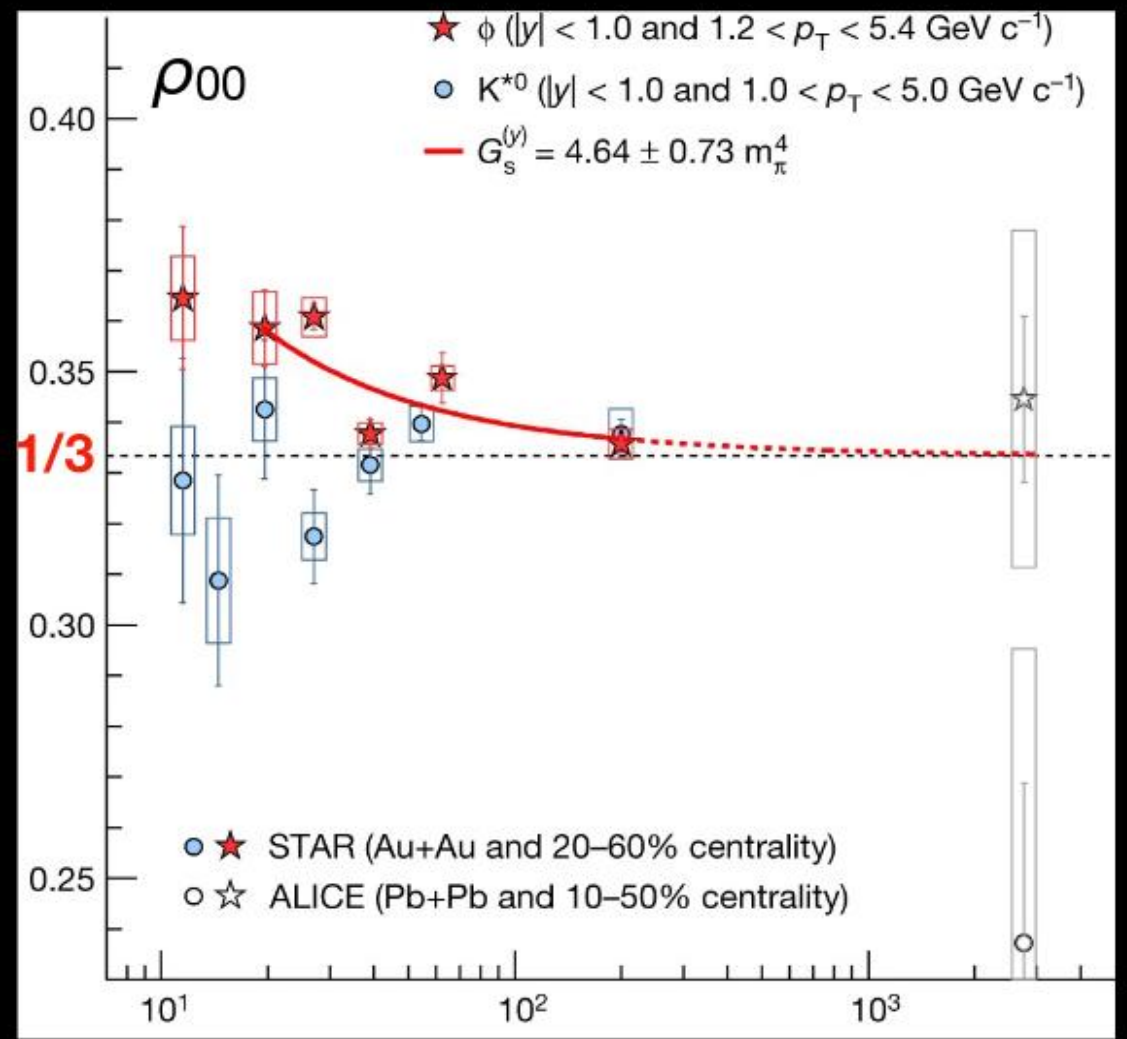
STAR: Nature
<https://www.nature.com/articles/s41586-022-05557-5>

Vector meson



$$\frac{dN}{d(\cos\theta^*)} \propto (1 - \rho_{00}) + (3\rho_{00} - 1)\cos^2\theta^*$$

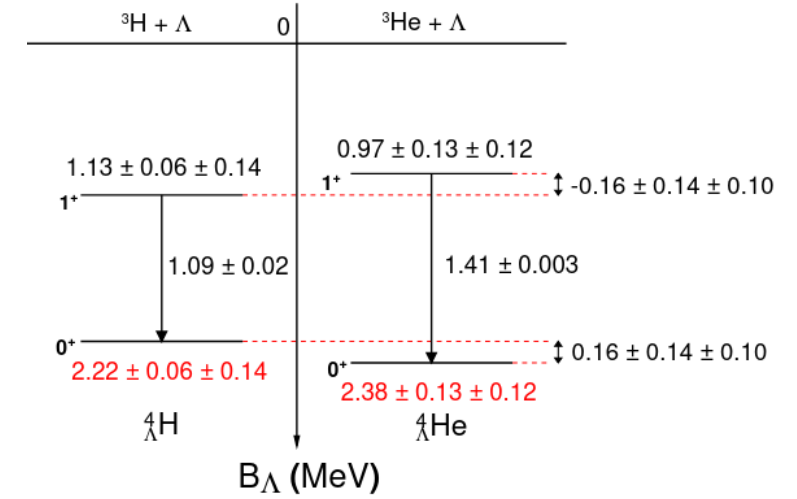
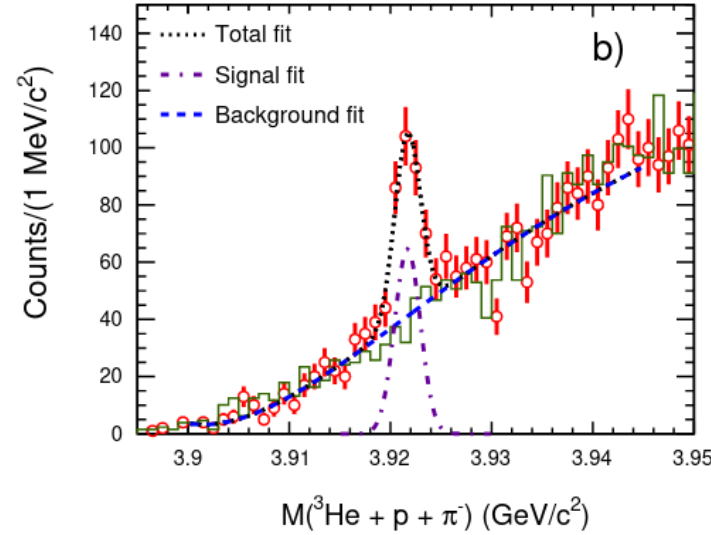
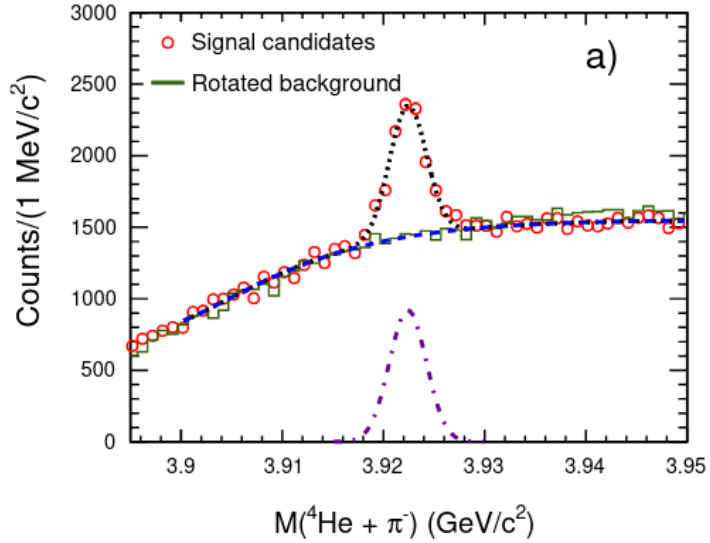
Possible explanation of this deviation for ϕ -spin alignment from $1/3 \rightarrow$ vector meson field



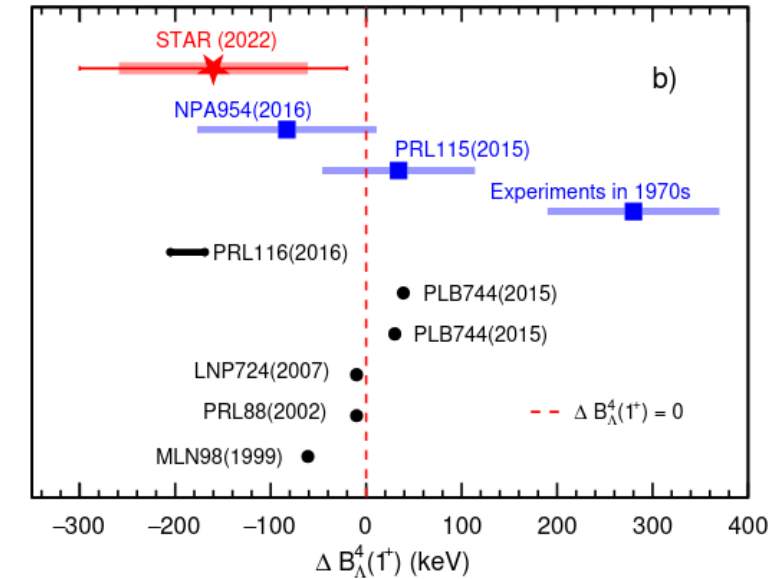
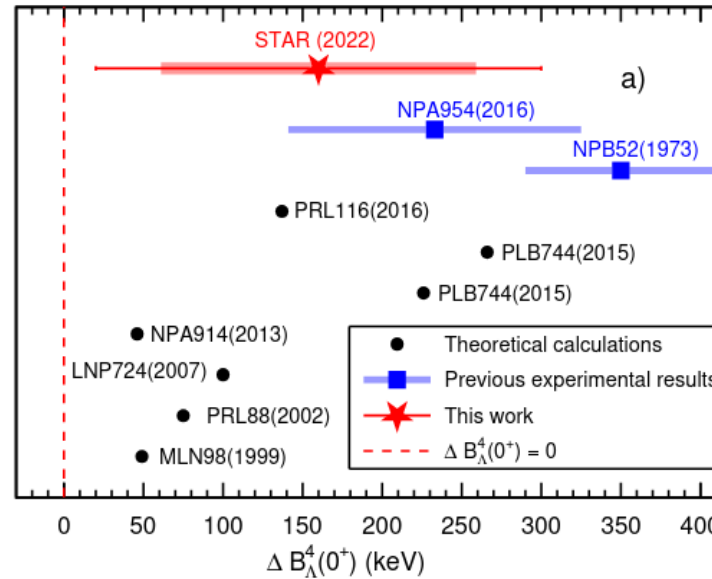
STAR $^4_{\Lambda}\text{H}$ and $^4_{\Lambda}\text{He}$ binding energy in Au+Au collisions at $\sqrt{s_{\text{NN}}} = 3 \text{ GeV}$

Phys. Lett. B 834 (2022) 137449

$$B_{\Lambda} = (M_{\Lambda} + M_{\text{core}} - M_{\text{hypernucleus}})c^2$$



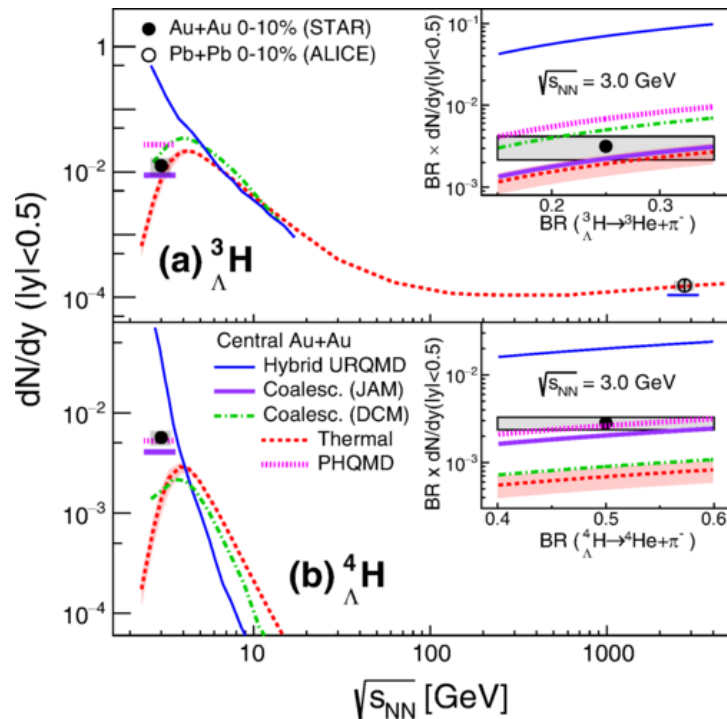
Phys. Lett. B 834 (2022) 137449



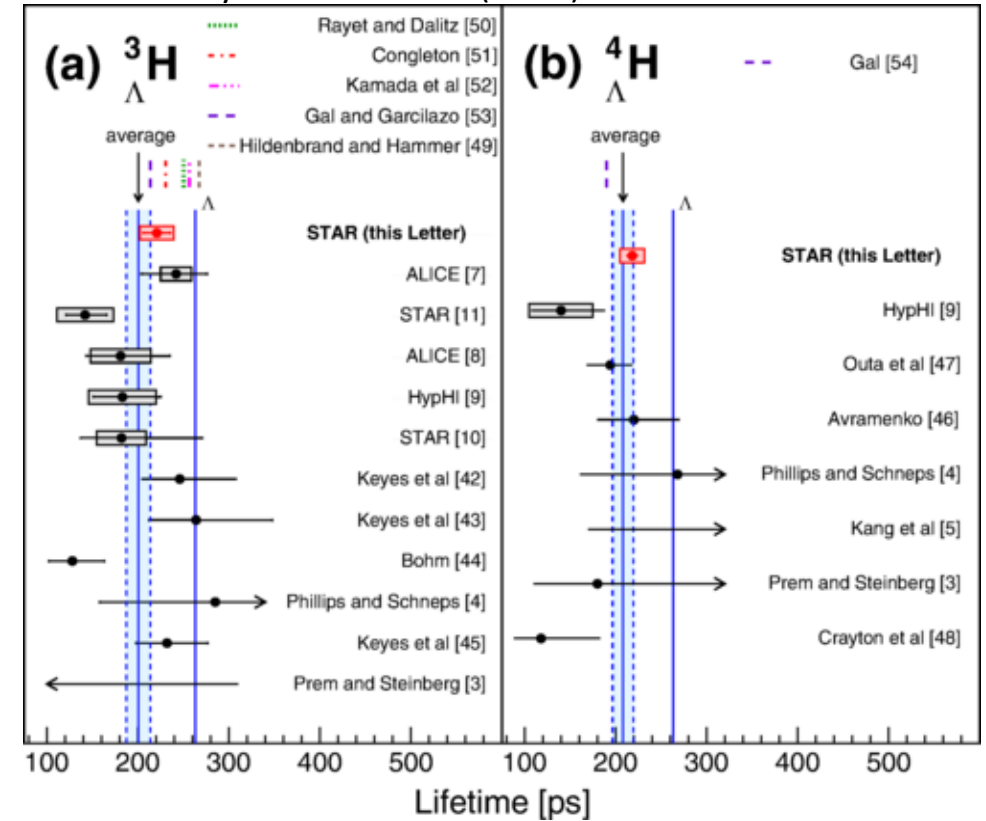
- Masses and the Λ binding energies of the mirror hypernuclei, $^4_{\Lambda}\text{H}$ and $^4_{\Lambda}\text{He}$, are measured in Au+Au collisions at $\sqrt{s_{\text{NN}}} = 3 \text{ GeV}$.
- By using the γ -ray transition energies of the excited states from previous measurements

STAR ☆ ${}^3_{\Lambda}\text{H}$ and ${}^4_{\Lambda}\text{H}$ lifetimes and yields in Au+Au collisions at $\sqrt{s_{NN}} = 3 \text{ GeV}$

- $\tau({}^3_{\Lambda}\text{H}) = 221 \pm 15(\text{stat.}) \pm 19(\text{syst.}) \text{ ps}$
 $\tau({}^4_{\Lambda}\text{H}) = 218 \pm 6(\text{stat.}) \pm 13(\text{syst.}) \text{ ps}$
- Calculations from the thermal model, which adopts the canonical ensemble for strangeness that is mandatory at low beam energies are compared to data
- Thermal model predictions are consistent with the ${}^3_{\Lambda}\text{H}$ yield, but underestimates the ${}^4_{\Lambda}\text{H}$ yield
- Hadronic transport models JAM and PHQMD calculations reproduce the measured midrapidity reasonably well

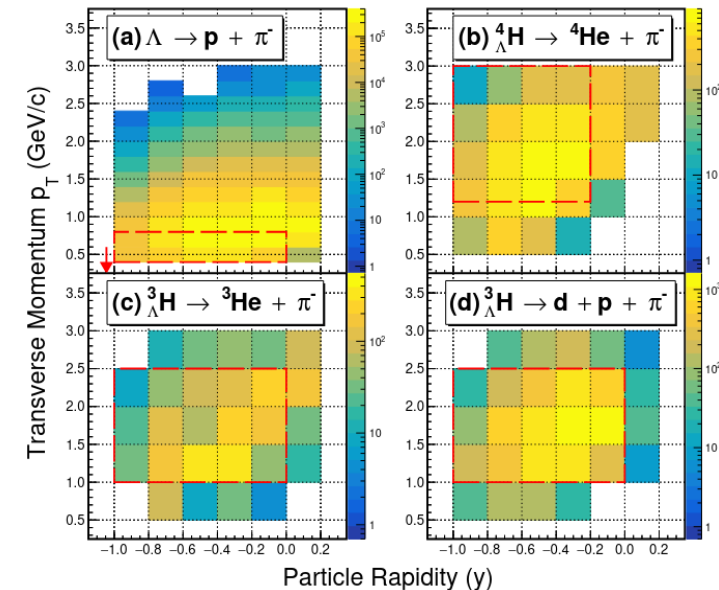
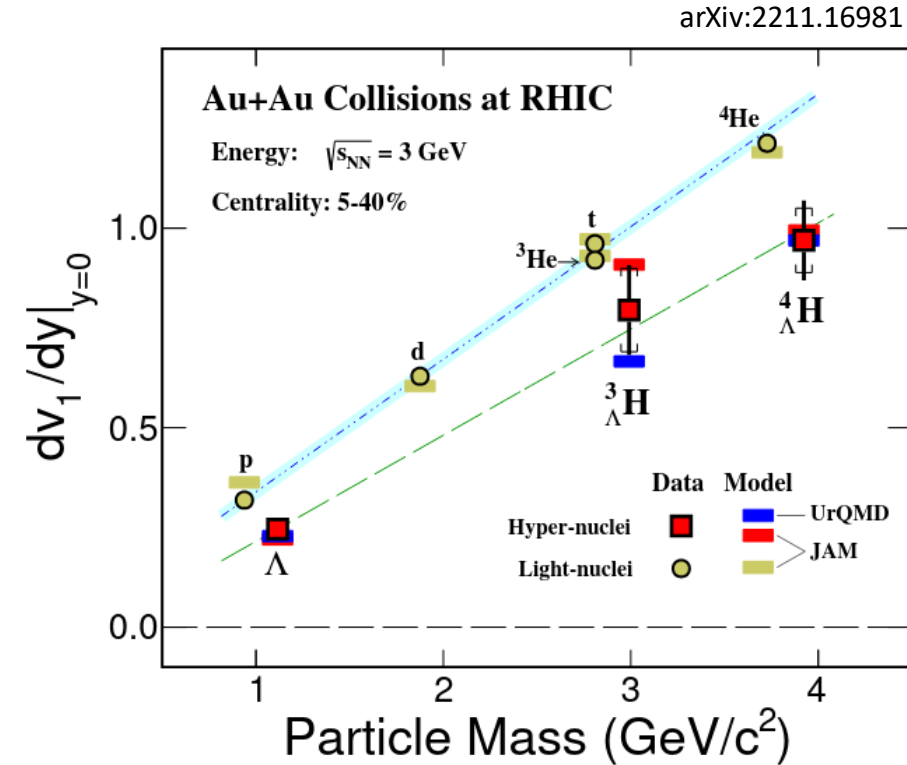
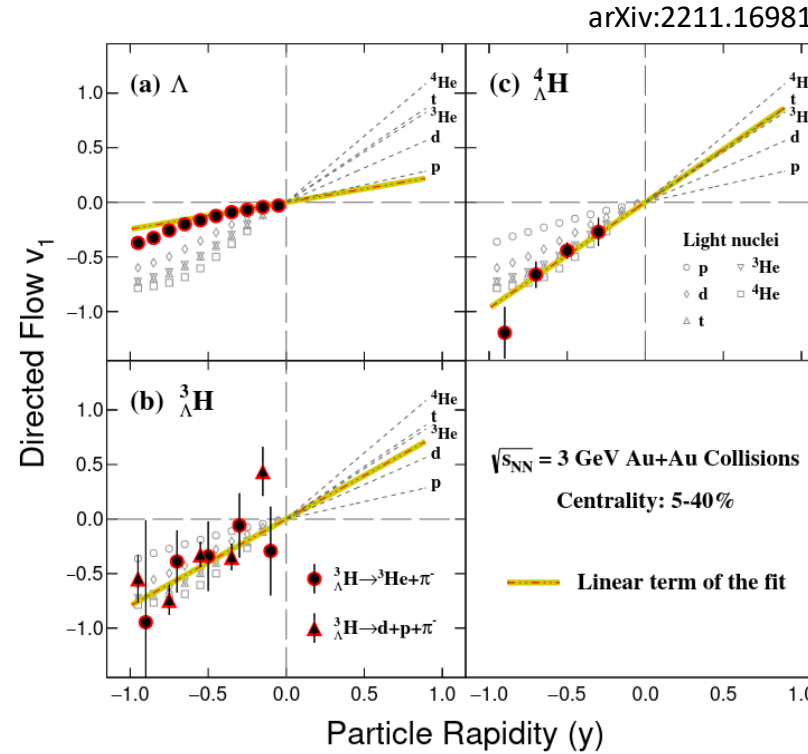
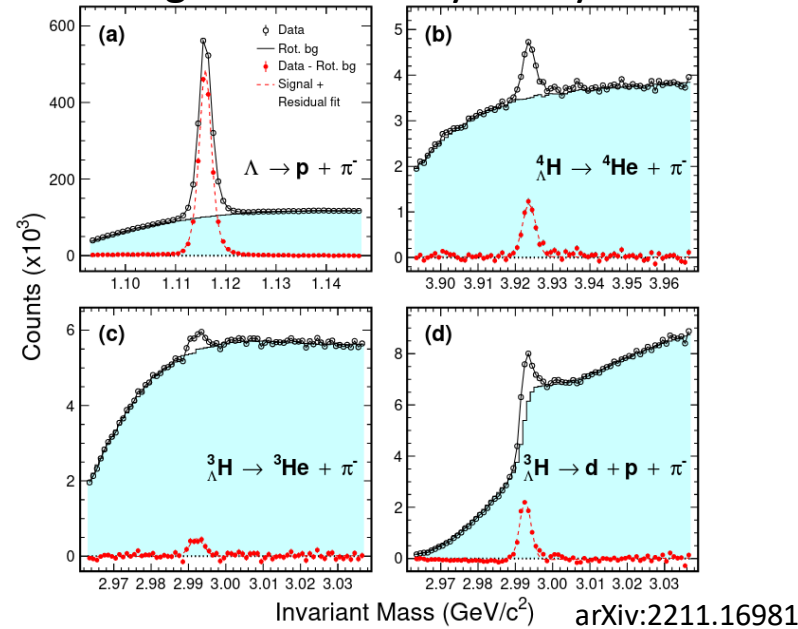


Phys. Rev. Lett. 128 (2022) 202301



STAR ☆ Hypernuclei flow

Utilizing 2- and 3-body decay channels



- About 280M events were analyzed. Almost 1.7B events will be produced soon.
- JAM and UrQMD plus coalescence afterburner calculations for hypernuclei are in agreement with data within uncertainties
- Data suggest that coalescence of nucleons and hyperon Λ could be the dominant mechanism for the hypernuclei ${}^3_{\Lambda}\text{H}$ and ${}^4_{\Lambda}\text{H}$ production in such collisions

STAR ☆ STAR 2023-2025 Run Plan and Physics Program

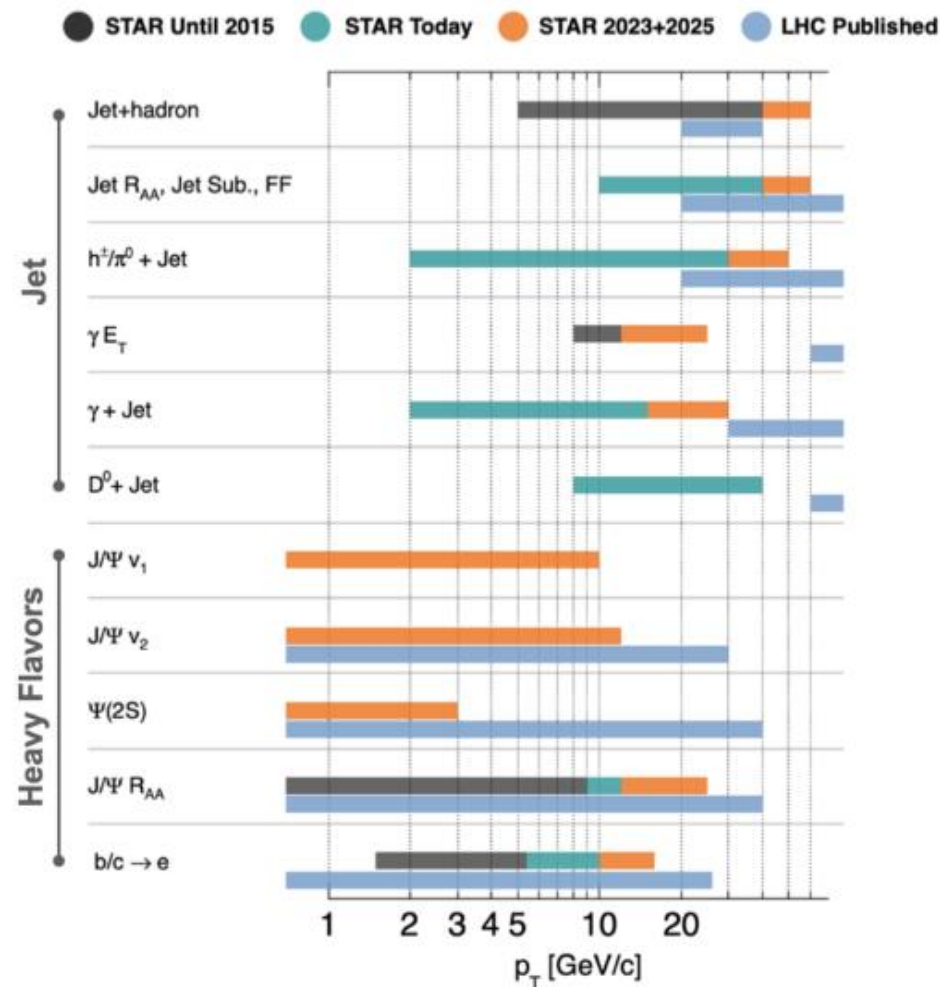
Run plan



It includes Hot-QCD and Cold-QCD STAR programs.

- Hot-QCD program: Study the microstructure of the QGP
Precision jet and heavy-flavor measurements

Kinematic coverage



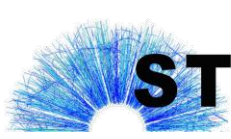
STAR ☆ Summary

- BES-II upgrades performing at or above expectation
- Excellent performance from RHIC and STAR
- All requested BES-II data collected, providing 17 unique energies from 3-200 GeV with some overlapping collider and FXT energies
- Precision analyses are ongoing with very well understood detector
- Most exciting features:
 - Rcp: change of the behavior at $\sqrt{s_{NN}} \sim 30$ GeV
 - Net-proton fluctuations: hints for criticality at $\sqrt{s_{NN}} \sim 17$ GeV
 - Correlation femtoscopy: peak structure at $\sqrt{s_{NN}} \sim 30$ GeV
 - Hypernuclei: many new measurements
 - Vorticity: from discovery to the precise measurements
- Many results exist and a lot more will come soon

From Sergei A. Voloshin

**PAY ATTENTION TO DETAILS: references, definitions and terminology,
clearly define physical goals and corresponding measurements/observables**

Backup



STAR ☆ Search for the Chiral Magnetic Effect (CME)

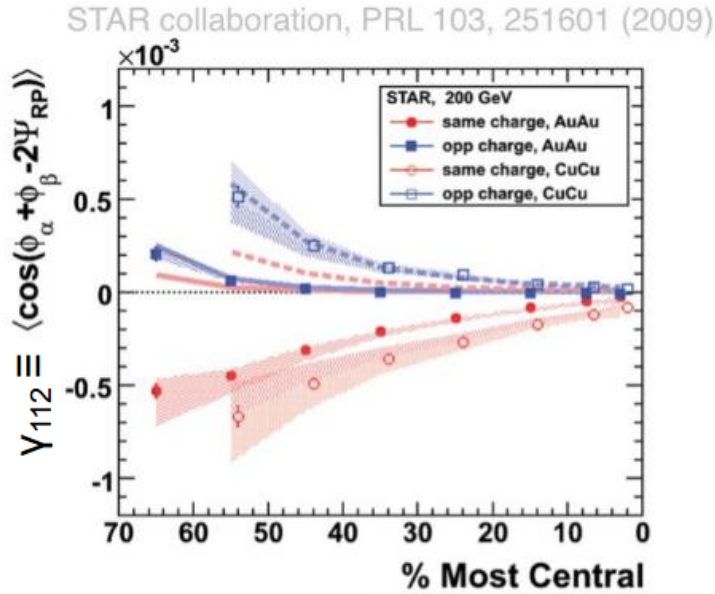
- The chiral magnetic effect (CME) is predicted to occur as a consequence of a local violation of P and CP symmetries of the strong interaction amidst a strong electromagnetic field generated in relativistic heavy-ion collisions.
- Experimental manifestation of the CME involves a separation of positively and negatively charged hadrons along the direction of the magnetic field.
- Previous measurements of the CME-sensitive charge-separation observables remain inconclusive because of large background contributions.
- In order to better control the influence of signal and backgrounds, the STAR Collaboration performed **a blind analysis** of a large data sample **of** approximately 3.8 billion **isobar collisions of $^{96}\text{Ru}+^{96}\text{Ru}$ and $^{96}\text{Zr}+^{96}\text{Zr}$ at $v_{\text{NN}} = 200$ GeV.**

[arXiv:2109.00131](https://arxiv.org/abs/2109.00131)

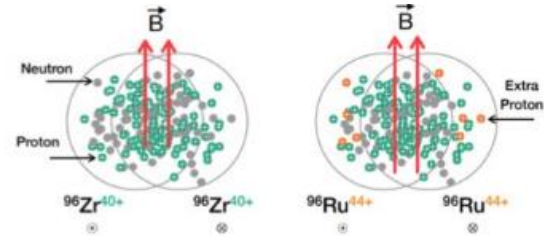
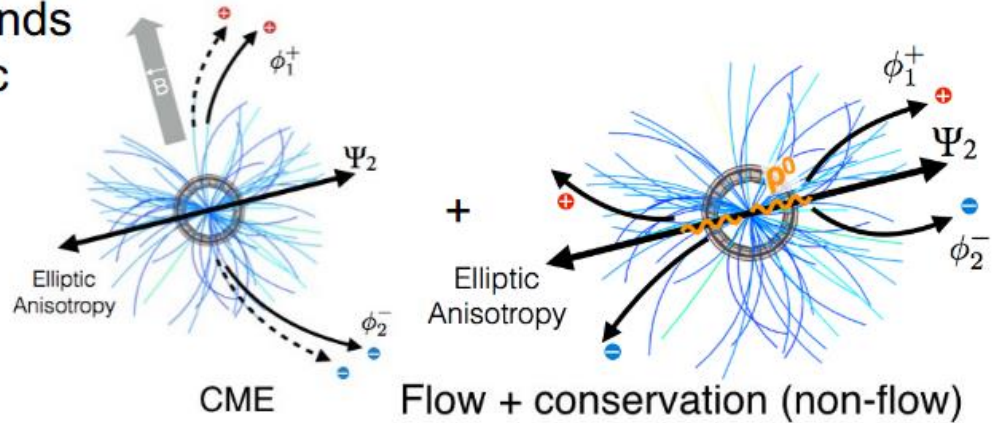
STAR ☆ Search for the CME (History)

First measurements

$$\Delta Y_{112} = Y_{112}^{\text{Opposite Charge}} - Y_{112}^{\text{Same Charge}}$$



Backgrounds can mimic signal

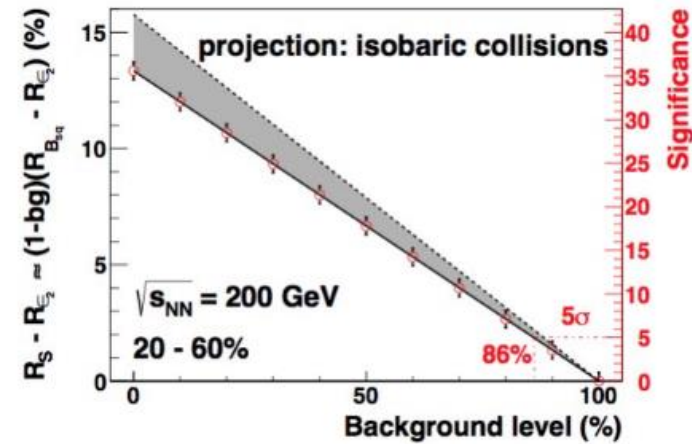


$$\Delta Y^{Ru+Ru} = \Delta Y^{CME} + k \frac{v_2}{N} + \Delta Y^{non-flow}$$

$$\Delta Y^{Zr+Zr} = \Delta Y^{CME} + k \frac{v_2}{N} + \Delta Y^{non-flow}$$

From B-field
10-18% different

Isobar idea:
Change signal while keeping background fixed



2018 Beam Use Request: Would see signal if background contributed up to ~80-85% to measure

Previous measurements of the CME-sensitive charge-separation observables remain inconclusive because of large background contributions.

STAR ☆ Search for the CME (Precision)

Large data set needed to hit small statistical uncertainty target

Systematic uncertainties between species need to be controlled below that level

Special RHIC conditions See G. Marr et al., in 10th International Particle Accelerator Conference (2019) pp. 28–32

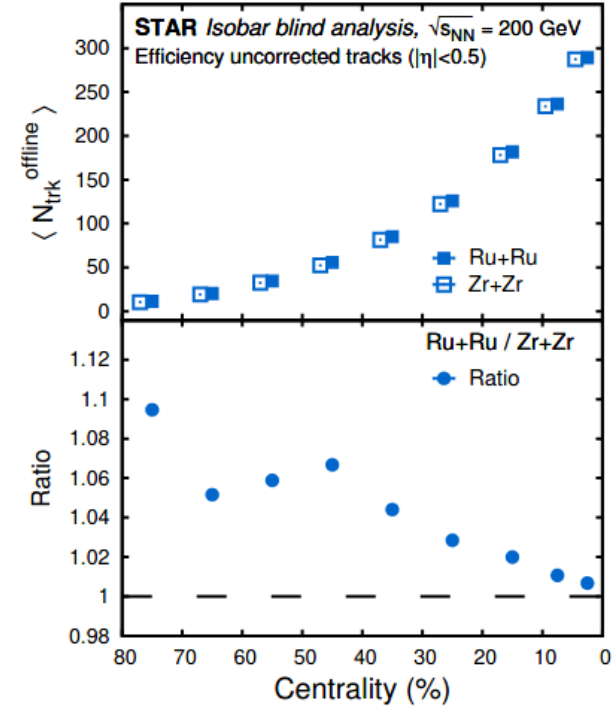
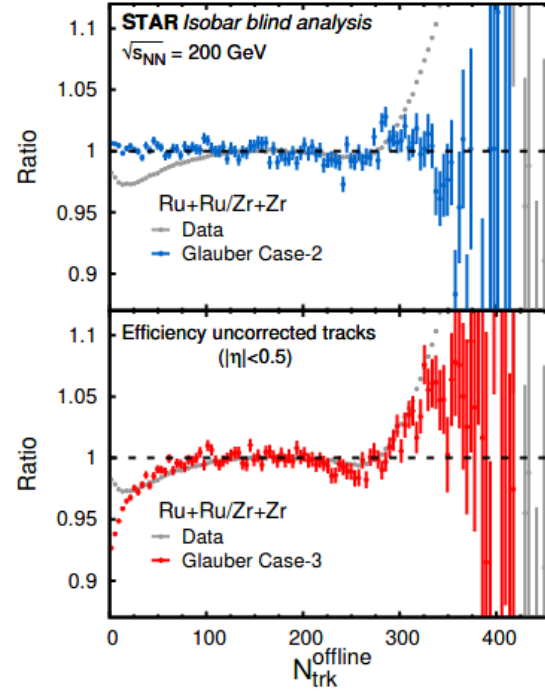
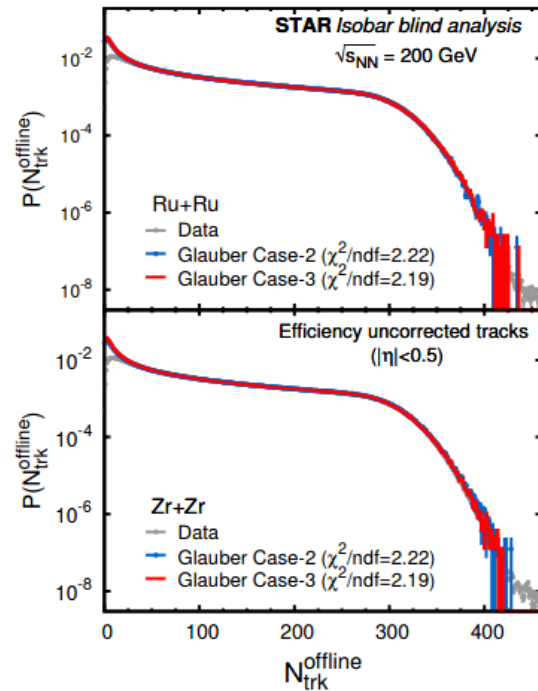
1. Alternate the isobar species between each store of beam in RHIC
2. Keep long stores with constant beam luminosity
3. Match luminosities between the species
4. Adjust the luminosity in such a way that the hadronic interaction rate at STAR is close to 10 kHz.

Precision target achieved:

A precision down to 0.4% is achieved, as anticipated, in the relative magnitudes of the pertinent observables between the two isobar systems

STAR Search for the CME (Centrality)

[arXiv:2109.00131](https://arxiv.org/abs/2109.00131)

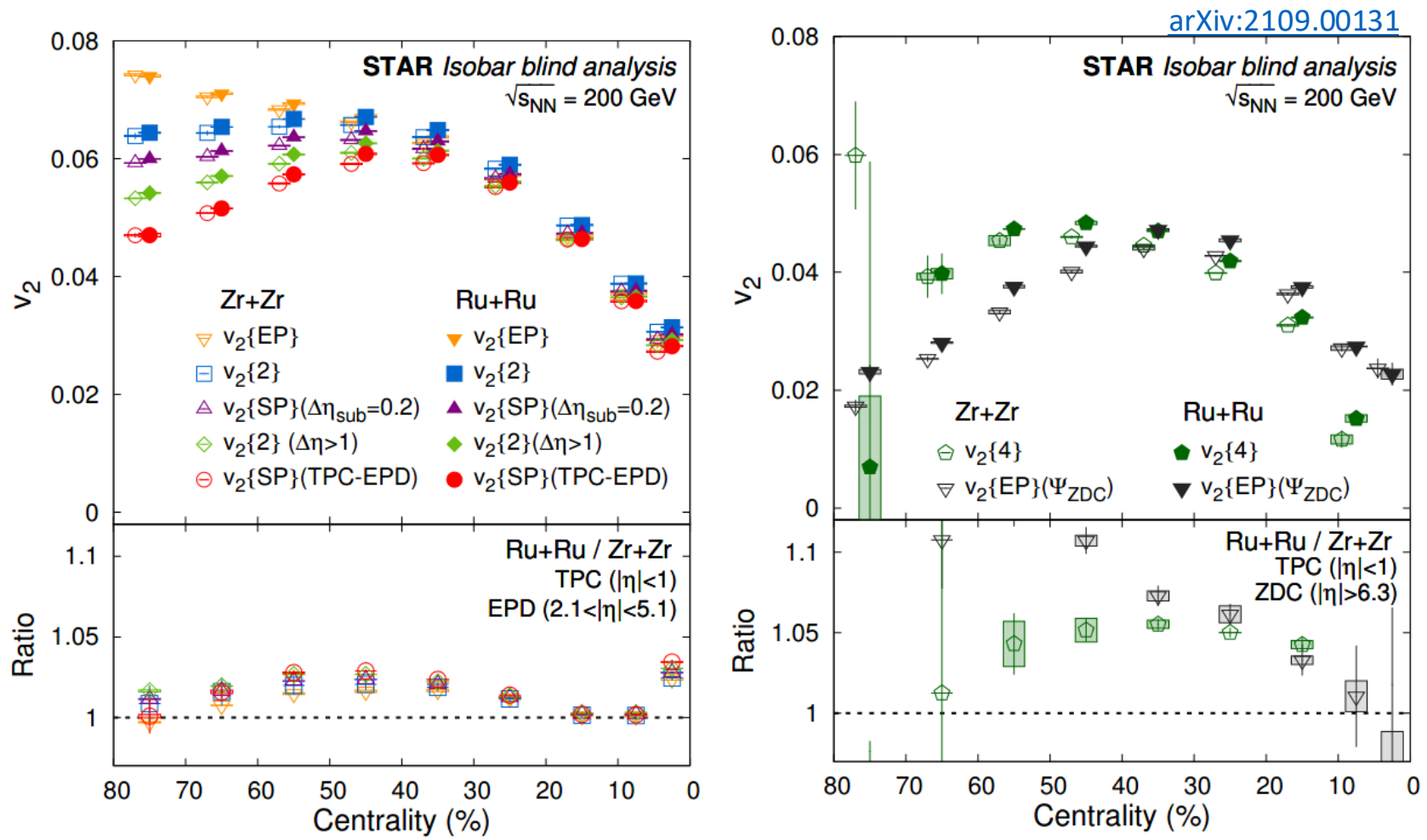


- The 3 sets of Woods-Saxon parameters from the literature have been studied
 - Fit to the multiplicity distributions using the two-component nucleon-based Monte Carlo Glauber
 - Best fit from Case-3: different neutron skin without quadrupole moments

Nucleus	Case-1 [83]			Case-2 [83]			Case-3 [113]		
	R (fm)	a (fm)	β_2	R (fm)	a (fm)	β_2	R (fm)	a (fm)	β_2
$^{96}_{44}\text{Ru}$	5.085	0.46	0.158	5.085	0.46	0.053	5.067	0.500	0
$^{96}_{40}\text{Zr}$	5.02	0.46	0.08	5.02	0.46	0.217	4.965	0.556	0

- Result: difference in multiplicity at matching centrality

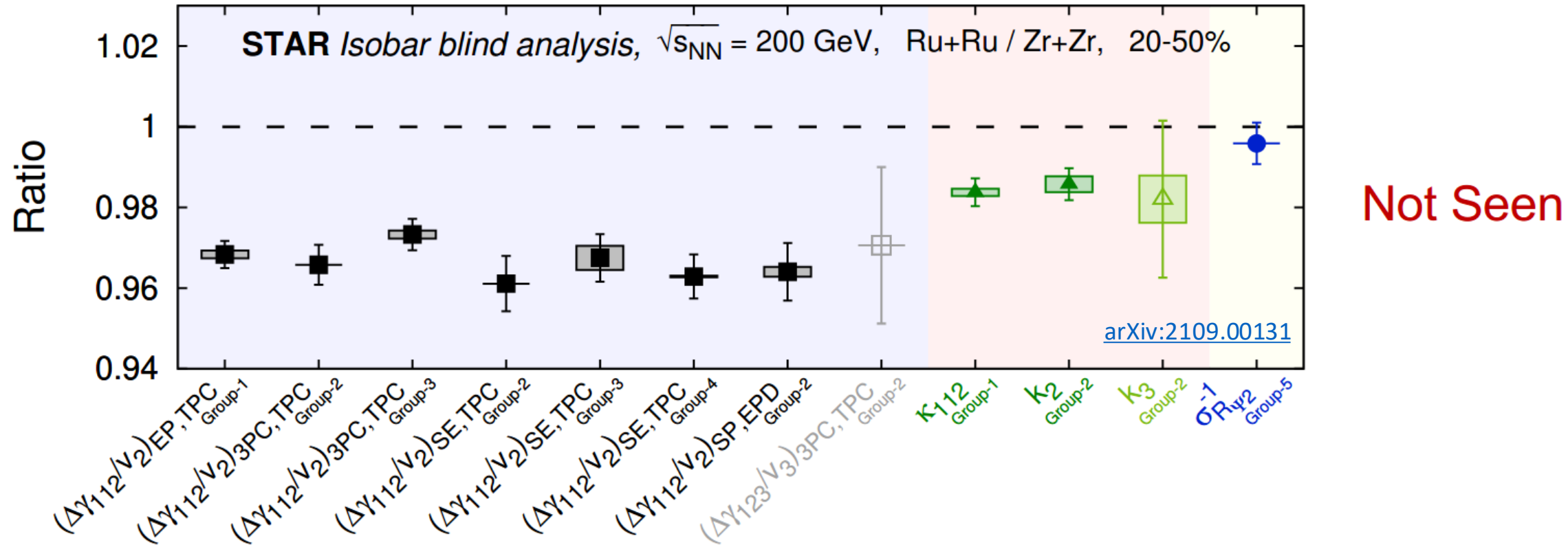
STAR Search for the CME (Crosschecks)



Observed differences in the multiplicity and flow harmonics at the matching centrality suggest that the magnitude of the CME background is different between the two species

STAR ☆ Search for the CME (Results)

Predefined CME signatures: ratios involving $\Psi_2 >$ those involving Ψ_3 , and > 1



No CME signature that satisfies the predefined criteria observed

Note: other measurements in paper that I don't have time to show in this talk

(spectator-participant analysis for CME signal fraction, $\Delta\eta$ dependence of correlations, ...):

All come to this conclusion